METHOD DEVELOPMENT FOR ELEMENTAL ANALYSIS IN FOODS AND PHARMACEUTICAL PRODUCTS USING X-RAY FLUORESCENCE

By

David Ochieng Wamwende

Submitted in Partial Fulfillment of the Requirements for the Degree of Master of Science in Chemistry

Youngstown State University

May 2023

METHOD DEVELOPMENT FOR ELEMENTAL ANALYSIS IN FOODS AND PHARMACEUTICAL PRODUCTS USING X-RAY FLUORESCENCE

David O. Wamwende

Signature

_____

David Ochieng Wamwende, Student Date.

Approvals:

_____

Dr. Josef B. Simeonsson, Thesis Advisor Date.

_____

Dr. Clovis A. Linkous, Committee Member Date.

_____

Dr. Ganesaratnam K. Balendiran, Committee Member Date.

_____

Dr. Sal Sanders, Dean of College of Graduate Studies Date.

ABSTRACT

General food and pharmaceutical analysis guidelines have been improved by the United States Pharmacopeia (USP) over the years to help in ensuring the quality, safety, and usefulness of products.

Atomic Spectroscopy (AAS, AES and AFS) has been used in sample analysis. These techniques have low detection limits, are precise and can provide reliable information. However, they involve complex sample preparation procedures and expensive reagents required for sample preparations and to maintain the instrument. It is important to develop a method that can be used to directly screen the samples during the production process and do not destroy the matrix. XRF is not destructive, fast process that does not involve a complex sample preparation procedure. The sample screen can be returned to the production conveyer, eliminating waste, and saving time. In our work we developed analytical methods for pharmaceutical and food samples. In the method the samples were analyzed directly with their matrix embedded. The results were cleaned of interferences using background interference corrections as well as fundamentals of Compton scattering techniques. Our analytes were Mn, Fe, Co, Ni, Zn and Cr The detection limits for these analytes were Mn (1 ppm), Fe (1 ppm), Co (1 ppm), Ni (1 ppm), Zn (4 ppm) and Cr (0.05 ppm)

ACKNOWLEDGEMENTS

I thank God who has been my rock and pillar throughout the journey.

I also register my most honest gratitude to my research advisor and mentor, Dr. Josef B. Siomeonsson for his continuous and tirelessly supporting my research by giving excellent directions throughout the course of my research. His directions and guidance have helped me throughout my entire research period and in drafting this thesis.

I also sincerely acknowledge my committee; Dr. Clovis A. Linkous and Dr. Ganesaratnam K. Belandrian. They have not only provided valuable scholarly comments and guidance during my research work but also you have provided fatherly advice which has helped me with both emotional balance as well as academic excellence! Thank you so much!

I also thank my colleagues in the lab: Van Nguyen; Samuel Ondieki; Zaire E Fabian; Cameron D Watkins. For helping me during my sample preparations as well as in running the samples.

I thank Ray Hoffs, for helping me with the instrumentation and troubleshooting the instrument in case of malfunctions.

The department of Chemical, Biological and Forensic Sciences and School of Graduate Studies, Youngstown State University has offered me financial support and providing the facilities and opportunity to do my graduate studies, thank you so much.

I finally thank my family for the everything they have provided me with and constant prayers throughout my whole journey.

TABLE OF CONTENTS

Contents

LIST OF FIGURES

LIST OF TABLES

LIST OF ABBREVIATIONS

ppm	Parts per millions
ppb	Parts per billions
ppt	Parts per trillions
XRF	X-Ray Fluorescence
Co	Cobalt
Fe	Iron
Mn	Manganese
Cr	Chromium
Pb	Lead
Bi	Bismuth
Zn	Zinc
LOD	Limits of Detection
LOQ	Limits of Quantification
ICP-MS	Inductively Coupled Plasma-Mass Spectrometry
USP	United States Pharmacopeia
ICP-OES	Inductively Coupled Plasma Atomic Emission Spectroscopy.
mL	Milliliters
KeV	Kilo electron volts
R	Rayleigh
C	Compton
R/C	Ratio of Rayleigh to Compton
USP	United States Pharmacopeia
AAS	Atomic Absorption Spectroscopy
AES	Atomic Emission Spectroscopy
AFS	Atomic fluorescence Spectroscopy
SCSPS	Signals in Counts Per Seconds
YSU	Youngstown State University
mm	Millimeters
Ar	Argon
eV	Electron Volts

INTRODUCTION

General food and pharmaceutical analysis guidelines have been improved by the United States Pharmacopeia (USP) over the years. The guidelines help in ensuring the quality, safety, and usefulness of the products.

In their guidelines, the following are reported with respect to X- Ray Fluorescence (XRF): USP 735, which is a guideline on XRF methodology; USP 232 for limits of elemental impurities; and USP 233 for toxicity analysis.

The long-term negative effects of impurities make them undesirable in pharmaceuticals and has led to extensive research to regulate organic impurities and residual solvents in pharmaceutical products. In addition to these impurities, there are class I and II (elemental) impurities which are metals and long-term use of products containing these impurities can have negative impacts. Some major sources of elemental impurities include contaminated raw materials, excipients, catalysts, and reagents introduced into the system during synthetic processes.

Previously elemental impurities have been detected and controlled using colorimetric tests. The methods involve non-specific heavy metal of all possible heavy metals. The sample colors are compared to the color of the solution, and this makes it hard to quantify the exact concentrations of the metals. This made it necessary to develop more accurate methods that can provide more reliable results. It is then those methods such as atomic spectroscopy were developed.

Atomic Spectroscopy

In atomic spectroscopy, atom analytes interact with radiation. For the information about the elemental content of the atom to be availed, a complete destruction of the sample is necessary. This renders the sample with inability to provide further information such as the character of the compounds present in the analyte.

Atomic Absorption Spectroscopy

The spectroscopy is based on three groups according to the free analyte-radiation interactions. These groups are Atomic Absorption spectroscopy (AAS). This applies principles that date back to as old as pre-1832, when Wollaston first observed the absorption lines spectrum from the sun. This principle was later explained by Brewster in 1832 (1). The low detection limit, precision, less operational sophistications in addition to minimal background errors has made the technique find operations in several laboratories.

The above advantages have made AAs find applications in many laboratories. Nonetheless the instrument is easy to operate and has fewer analytical interferences. However, there are several drawbacks from the AAS such as difficulty in handling solid samples and liquids of high viscosity directly. It is also hard to further dilute low concentration analytes and inconclusive results of oxides not affected by thermal variations.

Atomic Fluorescence Spectroscopy

AFS is an emission method which results from radiation which activates atomic vapor. This technique involves application of flame spectrometry in the analysis of samples. In this analytical technique, there is a total consumption of analytes into a flame of atomizer burner such as hydrogen in oxygen. There is excitation of the atoms at right angles to the optical exit, which is usually made of a monochromator of appropriate vapor lamps. It finds applications in flame cells for quantitative analysis of trace elements (2; 3).

Emission Spectroscopy

Atomic Emission Spectroscopy (AES) is a technique which includes sources consisting of flame as well as non-flame such as microwave plasma as well as Inductively couple Plasma is an example of AES (4; 3).

These techniques give more accurate and quantifiable results. These techniques included: ICP-MS and ICP-OES (5).

Why XRF?

The above spectroscopies provide detection limits as low as parts per billion and lower. However, they are costly and laborious and require a microwave or other digestion and chemical treatments, making the overall process complex. The use of oxidizing mineral acids to breakdown sample matrix is necessary and the generation of spectral interference can be caused by collision of the analytes and some common elements in the ICP MS plasma (proton, nitrogen 14, oxygen 16, argon 38 and argon 40). These interferences can make it difficult to accurately quantify a particular metal ion. (6)

Therefore, there is an important need to measure metals, especially hazardous metals, in a wide range of consumer products. The development of a fast and direct (or near direct) measurement procedure based on XRF would be much faster and more convenient for performing these measurements as compared to other instrumental methods that require samples that have been digested and put into solution (13).

The goal of the project is to further the development of a direct or direct analytical method based on XRF that can be used in the analysis of metals, including hazardous trace metals, in food, environmental, pharmaceutical and consumer products.

X- Rays

X rays have high photon energies and can pass through many types of materials. These objects include but are not limited to the human body and many solids.

In medical applications, they penetrate the body system and strike a detector on the other side of the body. In environmental and food applications, these radiations are used to determine concentrations of individual analytes in a sample.

Schematic diagram of X-Ray Fluorescence Process

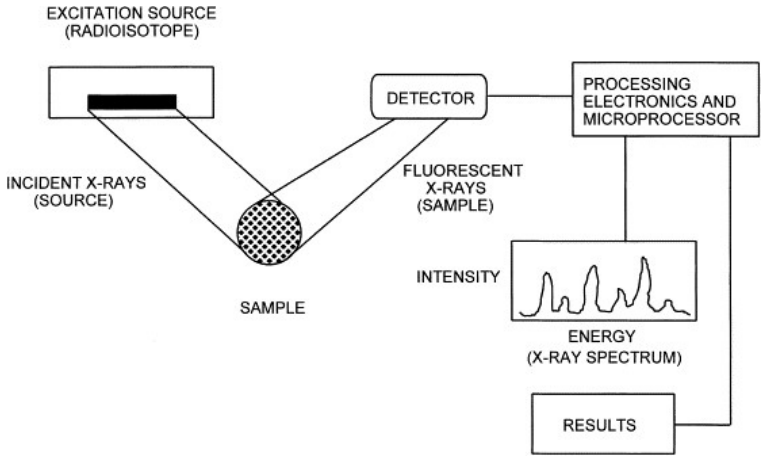

Figure 1 Schematic of X-Ray Fluorescence Process

(7)

Principles of XRF Process

The absorption of high energy X ray radiation causes the removal of an electron at the innermost orbitals. This excitation process is followed by a relaxation where outer electrons can relax to fill the inner shells and emit fluorescence radiation. This is a non-destructive process since the sample remains unchanged at the end of the fluorescence process. Each element has a distinctive range of energies where it emits fluorescence which allows each element to be measured selectively based on the photon energy (wavelength) of the fluorescence that is detected.

X-ray fluorescence instrumentation

The XRF instrument includes an x- ray tube that is necessary for atomic excitation in the sample. There is also a photon detector which is of tandem: ED XRF and WD XRF (8).

For elemental characterizations of samples, the S2 Ranger XRF was used which is in the Department of Chemical and Biological Sciences, Youngstown State University. This instrument is fitted with a palladium anode of 50 kV.

Sample types and holders

The samples to be analyzed include solid and solution standards used to prepare calibration curves. The sample holders are made using the XRF sample cups (SC-3340 40mm (about half the length of the long edge of a credit card) double open ended), from Premier Lab Supply, fitted with Spectro-Membranes Ultra- polyester Thin-Film (CAT. NO.:3090) from Complex Industries Limited, and membrane holder frames.

Detectors

There are three types of transducers used in modern instruments to improve on the early X-ray equipment that was based on photographic emulsions, which were slow and inaccurate. These are gas-filled, scintillation counters and semiconductor detectors, all of which employ a photon counting method in the processing of signals. In the photon counting approach, each electric pulse at the detector is produced by absorption of a quantum of X ray ramification which leads to the formation of electrons in the detector. The number of counts produced per given time are then recorded digitally as X ray photons. This technique is only applicable to a low intensity beam as multiple detector events that happen simultaneously can be mistakenly counted as a single event. In general, photon counting is ideal for spectra production without using a monochromator.

Ionization Chambers

These are operated in a range of voltage from V1 to V2. They employ a small current, usually between 10^-10 and 10^-16 A. The applied current also relies on applied energy. They lack sensitivity and are not applicable in X-ray spectrometry but have applications in radiochemical measurements.

Scintillation Counters

This was the earliest applied in zinc sulfide screening when the method involved the counting of individual flashes from individual photons manually. Gas filled detectors were developed to reduce the manual counting of flashes. These detectors were reliable, more convenient and gave valuable feedback to

radiation. This was further improved by the development of photomultiplier tubes. The most widely used has approximately 0.2% thallium iodide activated transparent sodium iodide crystal. It has a cylindrical shape and is about three inches cube. It is set in a manner that one of its plane surfaces to face the cathode tube. When incoming radiation goes through the crystal, there is a loss of energy to the scintillator which is subsequently given out in form of photons of specific wavelengths. The flashes produced in crystals are transmitted to the photocathode and are subsequently changed to pulses, magnified, and summed up. The photons produced is represent the energy of incident. For this reason, it is possible to analyze based on energy dispersive photomultipliers. Other organic scintillators are stilbene, anthracene and triphenyl. There are also organic liquid scintillators such as para terphenyl in toluene.

Semiconductor Detectors

These detectors work mostly with specialized instruments. They can respond to a wide range of photon energies, the most common being the Si detector. They can be fixed or movable depending on the type of instrument used. In general, the function of the detector is the conversion of the X-ray energy photons to pulse voltages. These pulse voltages can be counted and subsequently provide the total X-ray flux measurements. A narrow band is selected using voltage discrimination mechanism (7).

Inductively coupled Plasma- Mass Spectrometry

Principles

This instrument is used to measure and locate the elements imbedded in a sample matrix. The operation is based on the ionization of the elements within the sample. The ions are then separated and identified by mass spectrometry, after going through the ICP. By counting the number of selected analytes, the detector will then ascertain the concentration of all the elements chosen. This happens by the detector counting the number of the selected ions per second. The samples with complex matrices such as soil and biological samples are often digested before running into the instrument. It is fundamental to use liquified sample solution in the ICP analysis. Once the sample is liquified then argon is used as a carrier gas. The function of argon is to convert the samples to aerosols. This enables the instrument to take in only the smallest sample droplets through the chamber into the argon plasma torch, which is responsible for the samples' dissolution and ionization. Thereafter, the ions are then extracted from the plasma by skimmer and interference cones and extraction lenses. From the lenses, there is a refining of the ion particles as they go through an off-axis ion lens. This is necessary for the removal of photons and neutral ions. This fundamentally reduces the background noise. Kinetic energy discrimination is responsible for

removing the polyatomic ions which act as interferences. The sample beam, on the other hand is responsible for removing the larger poly atomic ions that are lose energy faster than the analytes (9), (10)

Schematic diagram of ICP-MS Instrument

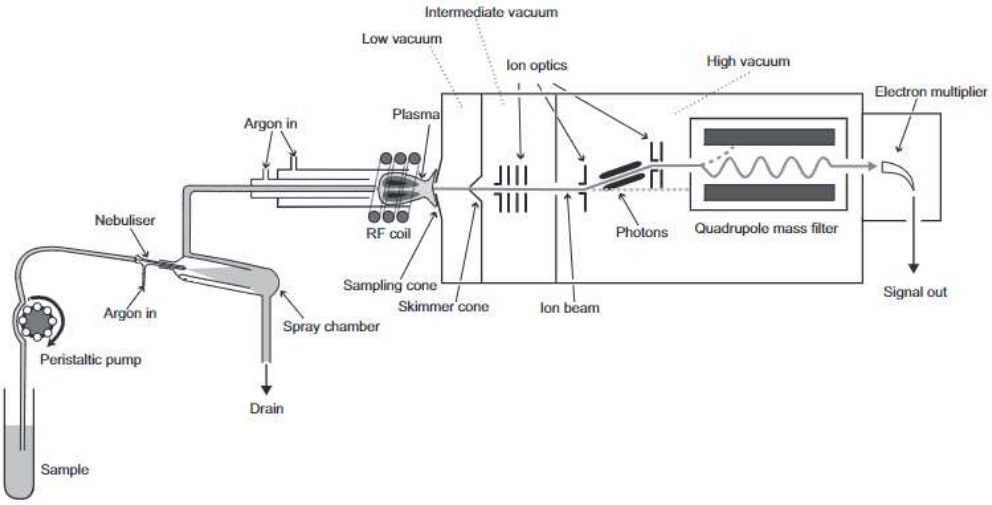

(11)

Figure 2 ICP MS instrument

Instrumentation

The instrument is designed to overcome several limitations for the analytical goal to be achieved. The argon source is combined with ICP source. This source has a magnetic sector analyzer with as well as several faraday cups. There is ionization at elevated temperatures with is usually 6000-8000k at the Argon plasma. This ionizes about 78% of the elements that have potential of less than 10 eV. It also has a magnetic sector mass analyzer. They operate with minimal transmission. This is achieved by incorporating a wide source and collector slits. The instrument also has mass bias which is corrected by use of stable isotope ratio measurements (12).

EXPERIMENTAL

Reagents and materials

The reagents of very high purity were used in the study in the analysis. A stock solution of the multi-element standard material was obtained from the standard 1000 ppm standard. From the solution, 12.5 mL was pipetted into a 50mL volumetric flask and diluted using deionized water to form a 250-ppm stock solution. The stock solution was appropriately diluted to prepare calibration standards. Mili q water was used for dilution. All the analytical balances used for measurements were calibrated according to Adriana *et al* 2012 guidelines on analytical balances calibrations (12).

Certified reference material and samples

A primary standard solution (multi-element IV-STOCK-4 1000ppm) was purchased from Inorganic Ventures; 300 Technology Dr., Christiansburg VA 24073 USA. Samples were purchased from local pharmacies and local food stores. All the instruments used were available at the department of chemical biological and forensic sciences here at YSU. The glassware was available at the quantitative analysis laboratory.

Sample preparations

Calibration standards preparations

All the sample preparation work was done before being taken to the instrumentation room for analysis. From the stock solution, 5mL was pipetted into a 10 mL volumetric flask and diluted using deionized water to form a homogenous solution to make 125 ppm concentration. From 125 ppm, 5 mL was pipetted into a 10 mL volumetric flask, to make 62.5 ppm concentration. From 62.5 ppm, 5 mL was pipetted into a 10 mL volumetric flask to make 31.25 ppm concentration. From 31.25 ppm, 5 mL was pipetted into a 10 mL flask, to make a 15.625 ppm solution.

Teas and coffee preparations

The coffee (Grev. D.R.), and tea used (oolong) were broken down to a powder using a pestle and mortar, and heated for one hour at 100 degrees Celsius to remove any available water contents (13)

ICP-MS Sample Preparations

Sample digestions

Several 50 mL volumetric flasks were gathered and cleaned of background metals by rinsing all the inside surfaces of each flask three (3) times with about 10 mL of a solution that is 1-part HNO3 and 10 parts milli

q water. After rinsing with the HNO_3 acid mixture, each flask was rinsed three (3) times with milli q water. Digestion of the tea leaves and other samples were performed by the following procedure: 0.5-gram mass of the sample was weighed out (on an analytical balance) and placed into a 50 mL beaker with 10 mL of concentrated HNO_3. (0.5396g Oolong tea; 0.5436g Ground cumin;0.5326g Ground cinnamon; 0.5414g Paprika; 0.5399g Acetaminophen; 0.5218g Ibuprofen; 0.5093Centrum; 0.5051g Tag lass Tea;0.5157g Green Tea and 0.5198g 1575A SRM).

The beakers with the sample/acid mixture were covered with an acid cleaned watch glass and the mixture boiled on a hot plate until the volume of the solutions was reduced to 2–3 mL.

The solutions were left to cool and then 10 mL of immersed HCl and 2 mL of H_2O_2 added to further assist digestion and the heating was continued on a hot plate until about 1 – 2 mL of samples were left.

The solutions were allowed to cool, about 30 mL of milli q water added and then the solutions transferred to 50 mL sample press vials.

The solutions were filtered in the sample vial using a 0.45-micron filter press, then transferred from the vial to an acid cleaned 50 mL volumetric flask. Any remaining solution was rinsed from the vial into the 50 mL flask using milli q water.

1 mL of concentrated HNO_3 was added to the solution in the flask and then diluted to exactly 50 mL using milli q water. The solutions were mixed well and then the sample solution mixture transferred to a new 50 mL sample vial. The solutions were capped with green plastic caps for storage until measurement by ICP-MS.

Calibration standards

The multielement standard solution (IV-STOCK 4) from Inorganic Ventures (shown above) containing each trace element at a concentration of 1000 ppm was used. The diluted calibration standard solutions were prepared in the five (5) 250 mL volumetric flasks.

The 250 mL flasks were rinsed with a dilute solution of HNO_3 acid in milli Q water before making the solutions (1-part concentrated acid to 20 parts water) to remove trace metal residues.

Then the flasks were rinsed at least three (3) times with milli Q water, and the flasks numbered 1 to 5 and the same flasks used each time for the same concentration.

The Following are the specific volumes and concentrations of standards prepared for each flask, where the dilutions for each flask were performed using milli q water Perform all dilutions using the milli q water. Flask 5: 2.00 mL of the IV-STOCK-4 solution pipetted and diluted to the mark to 250mL. 5mL HNO3 added to keep the acid concentration with the samples same. The final concentration of the elements was 8 ppm.

Flask 4: 4.00 mL of the Flask 5 solution was pipetted and diluted to the mark to 250mL. Final concentration of the elements is 128 ppb.
Flask 3: 3.00 mL of the Flask 5 solution was pipetted and diluted to the mark to 250mL. Final concentration of the elements is 96 ppb.
Flask 2: 2.00 mL of the Flask 5 solution was pipetted and diluted to the mark to 250mL. Final concentration of the elements is 64 ppb.
Flask 1: 1.00 mL of the Flask 5 solution was pipetted and diluted to the mark to 250mL. Final concentration of the elements is 32 ppb.
For calibration measurements, five (5) plastic sample tubes were prepared and approximately 40 mL of the following solutions transferred into the cups for individual measurements:

Sample 1 milli q water only (blank)

Sample 2 flask 1 solution

Sample 3 flask 2 solution

Sample 4 flask 3 solution

Sample 5 flask 4 solution

(14)

ICP MS measurements

The instrument was set on KED mode (kinetic energy discrimination) and all the samples measured using setting before making any changes to the instrument. For each solution, the instrument was set to perform 2 (two) survey scans and 3(three) analytical scans. The ICP-MS was set to measure all elements shown on the label of the IV-STOCK-4 solution.
Once the ICPMS data had been collected, it was saved the EXCEL or ".cvs" data files and transferred (imported) into Microsoft EXCEL for further data processing (15)

Sample cups and sample holders

The absorption of X-rays is determined by the sample holder's parameters such as thickness and the material compositions. For this reason, a Spectro membrane, made of Ultra-polyester thin film of diameter 76.2 mm, carried in thin film window carrier frame, CAT. NO.:3090, manufactured by Chemplex Industries INC., was used. This film had a gauge of 0.00006;1.5 micrometer; 15.240 Armstrong.

White sample caps, of 40 mm double open ended, manufactured by Premier Lab Supply SC-3340 were used.

Experimental setup

The prepared samples were weighed using analytical balance into sample cups, each sample approximately 5 grams. The samples were taken to S-2 Ranger XRF that uses helium gas as a coolant and palladium anode. The conditions were set as takeoff time of 90 seconds (about 1 and a half minutes), Incidence angle of 40 degrees and a running time of 488 seconds (about 8 minutes). The instrument was set to measure powder and liquid for standard solutions. The measurement was done in four ranges; 1, 2, 3 and 4. The results were extracted from the read out (desktop computer) where they were stored as dumped XRF results they were converted to a format that can be cleaned and analyzed using Microsoft office. The analysis was done and reported (16).

RESULTS AND DISCUSSIONS

S2 Ranger results

All XRF measurements were performed using the S2 Ranger instrument in the YSU Chemistry Department. The first set of XRF measurements were performed using the S2 Ranger instrument. Shown in Table 1 are the XRF photon energies that correspond to the elements that were measured (17)

The table of Analytes and their respective energies in kiloelectron volts.

Analyte	Cr	Mn	Fe	Co	Zn	Pb	Bi	Ni
E. keV	5.42	5.90	6.41	6.93	8.64	10.6	10.8	7.48

Table 1 Analytes and their respective energies

In XRF, the XRF spectral data can be used to identify each element and quantify the amount of the element that is present in the sample. Quantification has been performed using the method of calibration curves where a series of calibration standards containing investigated amounts of analytes are measured to obtain a calibration function in the form of a linear equation. Then the measured responses for the unknown samples are converted to concentrations using the calibration equation.

Solution standards

X-Ray fluorescence has been shown to incorporate both the liquid and the solution standard in elemental analysis in pharmaceuticals. This method used the solution standard in determination of Cobalt in solid pharmaceutical products. In the study the concentration of Co was determined in vitamin B12. It has also been reported that elevated background makes it difficult to analyze some elements using the approach (18). It is important to study if the same approach is applicable for non-pharmaceuticals such as cosmetics and food samples. The realization of this will provide a good foundation for industrial screening of the product's elemental contents for the purpose of speeding up the production chain by realizing the samples that have off the required elemental production limit. It has also been reported that Wavelength dispersive XRF provides a scientific instrument for the pharmaceutical industry for both pharmaceutical medicines as well as active molecules. It is therefore worth exploring the method with ED XRF and its applicability in non-pharmaceutical samples. (19).

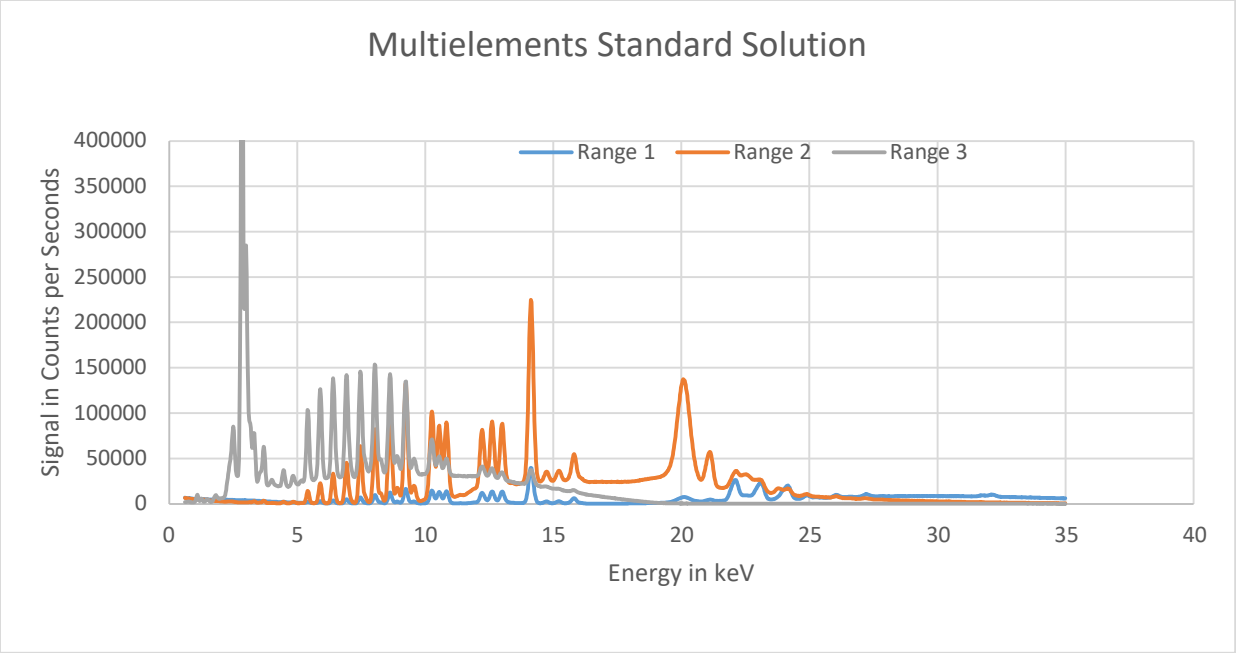

Figure 3 Multielement Solution Standard graph

Shown in Figure 3 is the XRF spectrum obtained for the multielement standard solution (IV- STOCK-4) from Inorganic ventures. This standard solution was used to prepare calibration standards for quantitative analysis of the samples. The standard provided XRF responses in three ranges; range 1 which uses copper filter, range 2 which uses aluminum filter and range three which is not filtered. The Compton and Rayleigh peaks have signals in ranges 1 and 2, with range 2 having the highest counts of the signal intensity per unit time. For this reason, the range 2 signals were used for the preparations of calibrations and all the analysis of the samples are based on the calibrations and range 2 responses (20)

Calculation of background corrected peak heights for each element.

Measurement errors caused by variations in the background intensity can be due to both matrix and instrumental interferences. The matrix effects result in background noise which cause the data to be inaccurate. This effect is corrected by measuring the height of the signal from the base and subtracting the height from the base of the shoulder of the signal peak. This corrects for errors due to background effects. (21). This was done for all the analytes, and results tabulated below, followed by preparation of the regression curves.

The Table of Background Corrected Peak heights.

	ppm	250	125	62.5	31.25	15.625
Analyte						
Mn		19458.5	7446.5	3831.5	1932.5	926
Co		40428	16682	8378	4214.5	1855
Ni		53974.5	23194.5	12148	6182	3823
Fe		30070.5	11421.5	6079	3407.5	1498.5
Pb	Background	45497.5	19371	10227.5	5641	2480
Bi	Corrected	62712	25181	13697	7316.5	3225.5
Cr		12005	4989.5	2424	1363	627
Zn		97759.5	40771	20952.5	11484.5	5012

Table 2 Background Corrected Peak Heights against Concentrations in parts per millions.

Shown below in Figures 4-8 are calibration curves for several elements where the background corrected peak intensities for the primary XRF peak for each element is plotted against known quantity in each standard. The way each of the plots show, the responses are linearly proportional for each element over the calibration range from 15-250 ppm.

Background Corrected Peak Height Curves for Mn, Co, Ni, Fe, Pb, Bi, Cr, and Zn.

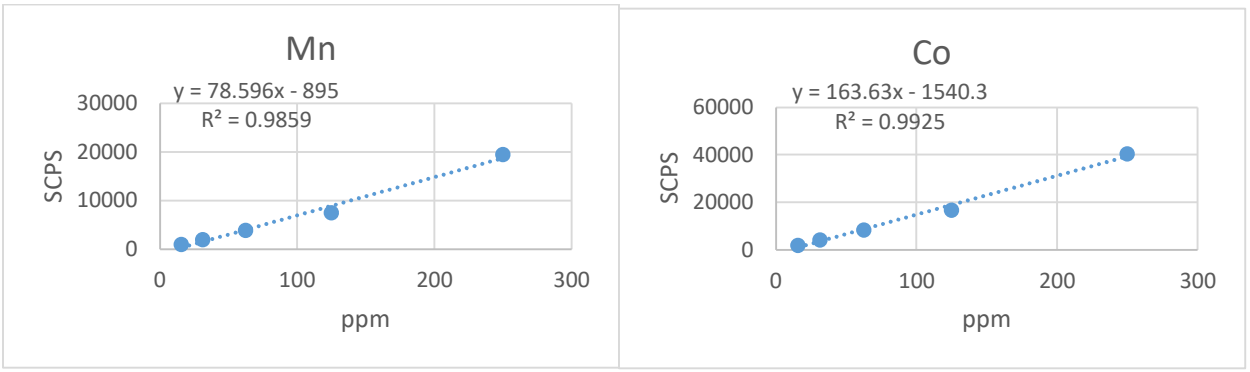

Figure 4 Background corrected linear regressions for Manganese and Cobalt peak heights.

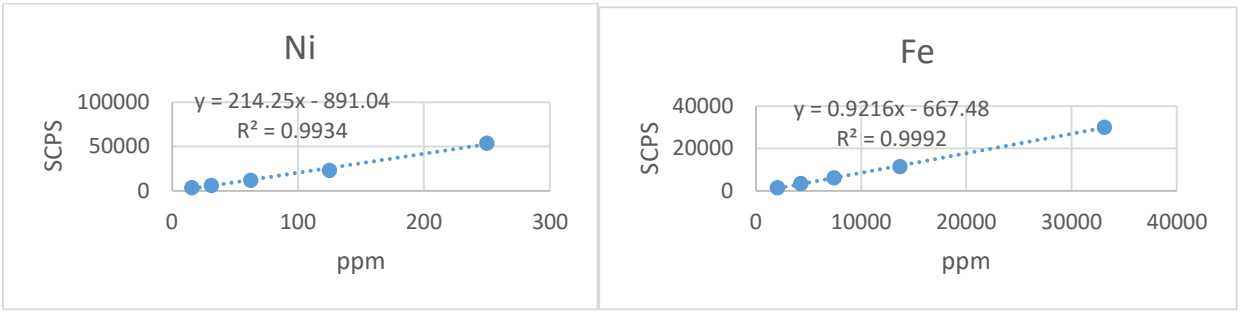

Figure 5 Background corrected linear regressions for Nickel and Iron peak heights.

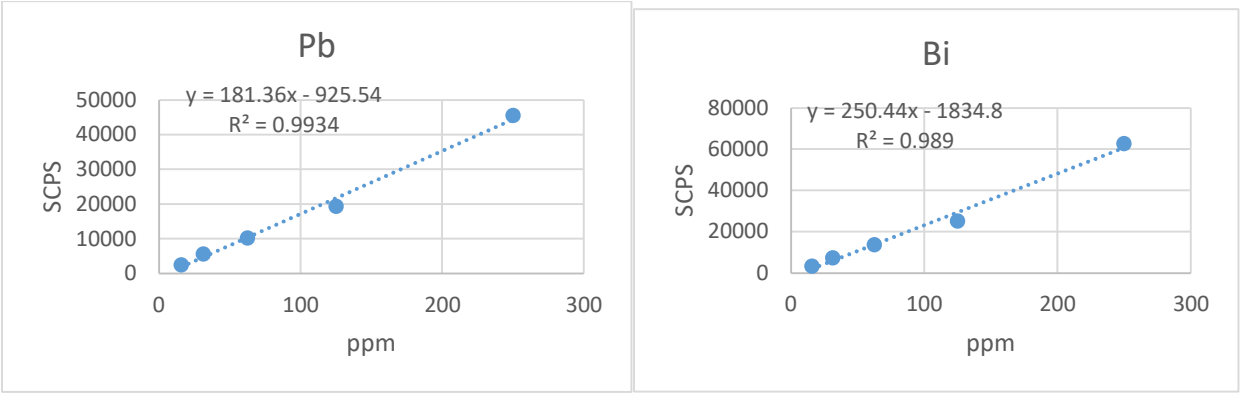

Figure 6 Background corrected linear regressions for Lead and Bismuth peak heights.

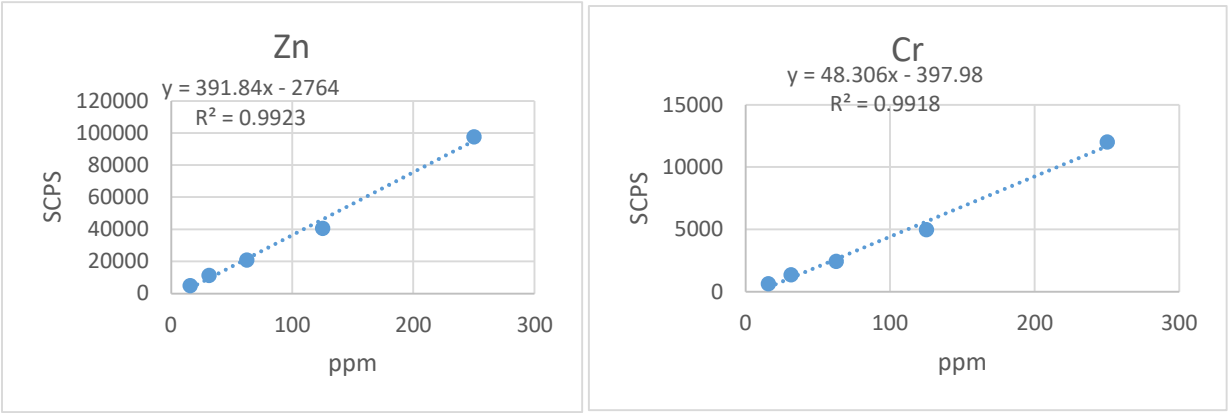

Figure 7 Background corrected linear regressions for Zinc and Chromium peak heights.

The approach gave an overall good correlation coefficient, but it is worth exploring other correction approached as suggested by P M S Carvalho et al, to improve the accuracy. It is therefore for this reason that other approaches are done to immunize inaccuracy as much as possible these methods are Compton correction approach as well as Rayleigh to Compton correction approaches (13)

Correction based on Compton.

In some cases, the linearity can be improved by using a correction factor on the Compton and Rayleigh scattering form the source of radiations (22). Compton peaks in the XRF spectrum are produced from the incoherent back scattering of the fluorescence from the source. This peak is produced always in every sample. Changes in the sample matrix cause its intensity to change.

The figure of the Compton peak

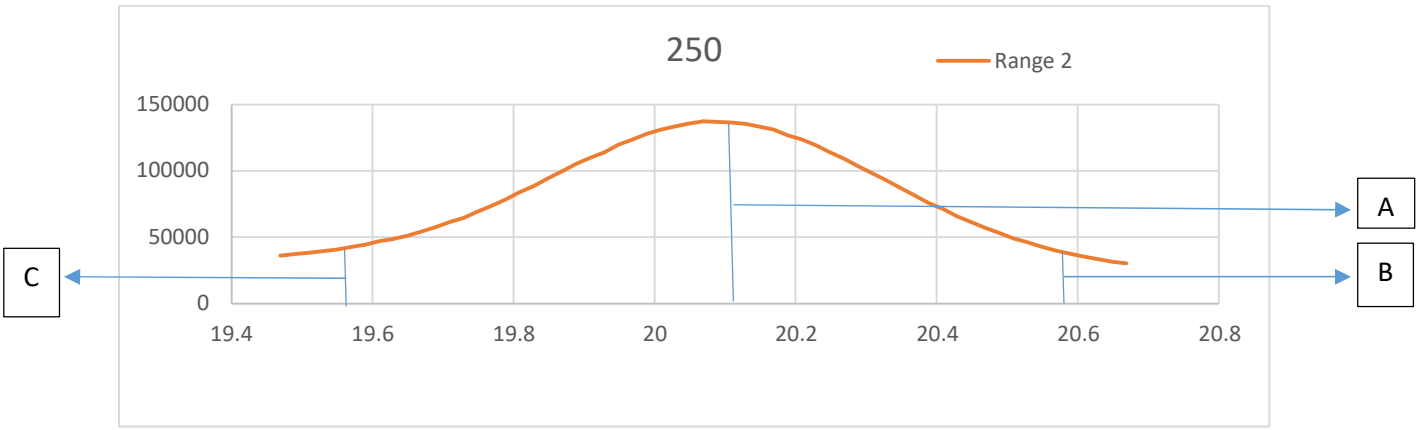

Figure 8 The Compton Peak

The Compton peak is produced in the Rh energy region, at 20.216 kilo alpha Kilo electron volts (17). The signal should ideally be a sharp line at the energy region, but this is not the case due to interference (16). This interference causes shouldering of the peak and background noise that should be subtracted from the peak to get the effective signal that can be measured and quantified. Using figure 9 above for illustrations both peak heights and peak areas were corrected as follows:

Peak Height

A is the signal plus background height, B and C are the individual shoulders of the peaks. B and C represent background interference. To have effective signals the background interference must be subtracted from the signal height represented by A, which includes the effective height and interference. The background is not always uniform throughout the signals and because of this, their average should be determined and subtracted from A. This can be represented mathematically as follows.

$$A - \frac{B + C}{2} = Effective\ Signal$$

Peak Area

The peak area is realized by taking the sum of the peak signals (23). This includes the signal peak and background area. The background interference is eliminated by taking the averages of the shoulder heights to give the background height. This background height is then multiplied by the distance between them. The product of the background height and distance between the peak's shoulders is the background area. This area is then subtracted from the sum of the signals to give the signal area, which is also called peak area. This can be illustrated mathematically as follows.

Corrected peak area$= \sum_{B}^{C}(signals) - Average[(C{:}\,B) * Energy\ Range\ (19.6\ to\ 20.6))]$

This operation is done in Microsoft Excel and the results are generated by Excel.

Matrices dominated by lighter elements produce a larger peak while the matrices dominated by heavier elements produce a smaller peak. Normalizing with Compton peak can reduce the nonlinearities from matrix effects (24)

The table of Corrections based on Compton Peak Heights

Concentration (ppm)	250	125	62.5	31.25	15.625
Compton (C)	101124	134002	142906	156779	155376
Rayleigh (R)	30138	36348	34246	40191	41239
R/C	0.298	0.271	0.25556	0.256	0.265

Table 3 Correlation correction based on Compton Peaks heights.

This method, however recommended by (24), did not work for my sample since the corrected signals, when corrected using Compton alone, become worse than when only background correction is done. Therefore, this method was not chosen as the overall method for the analysis of the unknowns. P M S Carvalho et al. used six approaches in their study based on fundamental parameters and external standard methods. They also realized that the method needed improvement.

Compton correction of background corrected peak heights for each element.

The background corrected signals were divided by their respective Compton peaks and contrary to what was expected, the regressions were worsened instead of improved. The table and subsequent data show the results from the Compton corrected peaks.

The Table of Peak Heights Corrected according to Compton.

	ppm	250	125	62.5	31.25	15.625
Analyte						
Mn		0.1924	0.05557	0.02681	0.01232	0.00595
Co		0.39978	0.12449	0.05862	0.02688	0.011193
Ni		0.53374	0.173	0.085	0.0394	0.0246
Fe		0.7345	0.2325	0.1095	0.0532	0.0246
Pb	Ratios of	0.4499	0.14455	0.071568	0.03598	0.01596
Bi	Peak height	0.62014	0.1879	0.0958	0.046667	0.020758
Zn		0.966728	0.304256	0.146617	0.073252	0.032257
Cr		0.1187	0.037234	0.01696	0.00869	0.004035

Table 4 Peak Heights Corrected according to Compton Corrections peak heights.

Compton Corrected Peak Height Curves for Mn, Co, Ni, Fe, Pb, Bi, Cr, and Zn

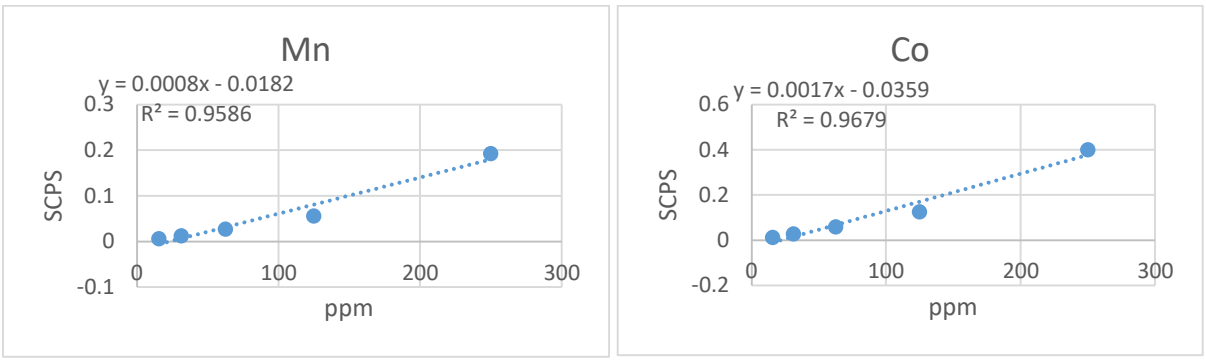

Figure 9 Compton corrected linear regressions for manganese and cobalt peak heights.

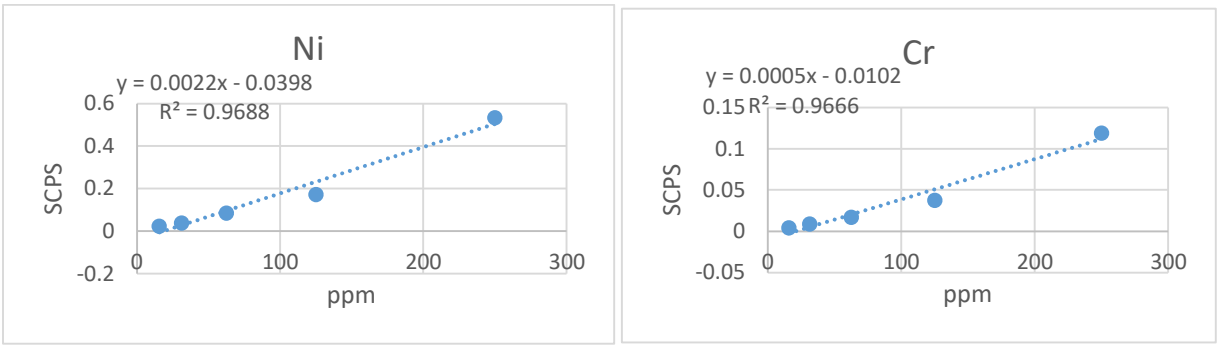

Figure 10 Compton corrected linear regressions for nickel and chromium peak heights.

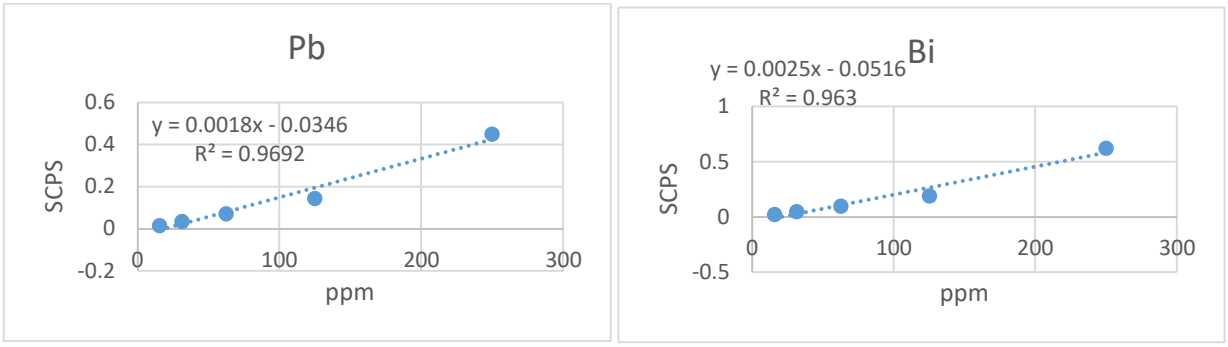

Figure 11 Compton corrected linear regressions for lead and bismuth peak heights.

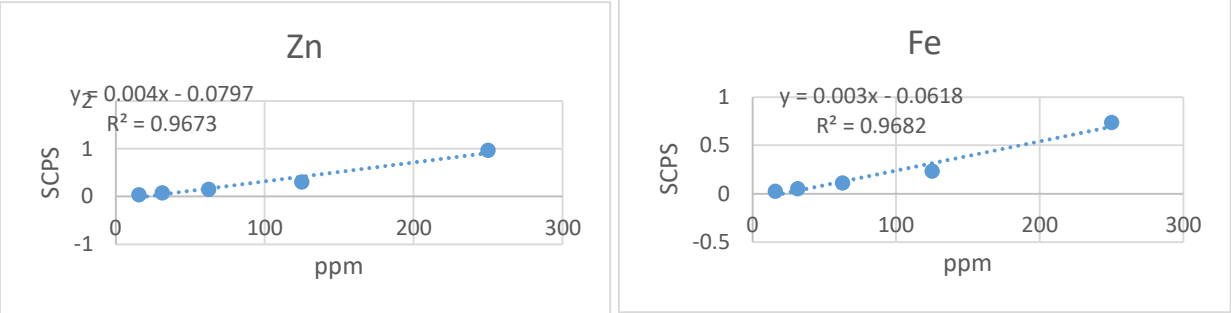

Figure 12Compton corrected linear regressions for zinc and iron peak heights.

Correction of background corrected peak heights with Rayleigh to Compton ratios.

The corrections were further investigated by dividing the background corrected peak areas with Rayleigh(R) to Compton (C) ratios, improving the regression data. The data were tabulated and recorded and are shown in the table below. The regressions were also made and recorded (6)

The Table of Rayleigh to Compton Corrected Peak Heights

	ppm	250	125	62.5	31.25	15.625
Analyte						
Mn		65296.97987	27477.85978	14992.56535	7548.828125	3494.339623
Co		135664.4295	61557.19557	32782.9012	16462.89063	7000
Ni		181122.4832	85588.56089	47534.82548	24148.4375	14426.41599
Fe		249278.5235	114983.3948	61236.10894	32638.67188	14445.28302
Pb	Peak	152676.1745	71479.7048	40017.95617	22035.15625	9358.490566
Bi	Height	210442.953	92918.81919	53596.02442	28580.07813	12171.69811
	To (R/C)					
Zn		328052.0134	150446.4945	81986.61762	44861.32813	18913.20755
Cr		40285.2349	18411.43911	9485.052434	5441.40625	2366.037736

Table 5 Peak Height Corrected according to Rayleigh to Compton Ratios Corrections

Rayleigh to Compton Corrected Peak Height Curves for Mn, Co, Ni, Fe, Pb, Bi, Cr, and Zn

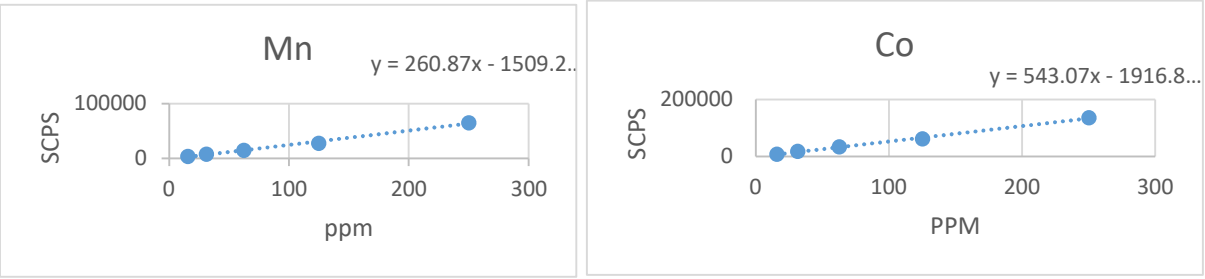

Figure 13 Rayleigh to Compton ratio corrected linear regressions for manganese and cobalt peak heights.

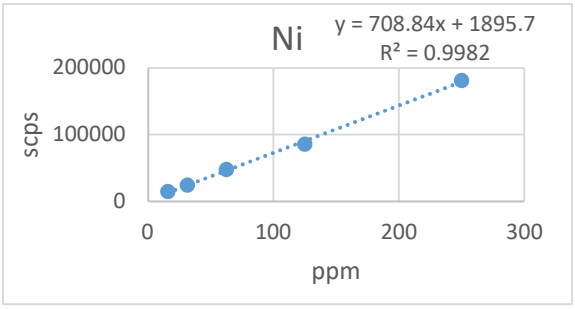

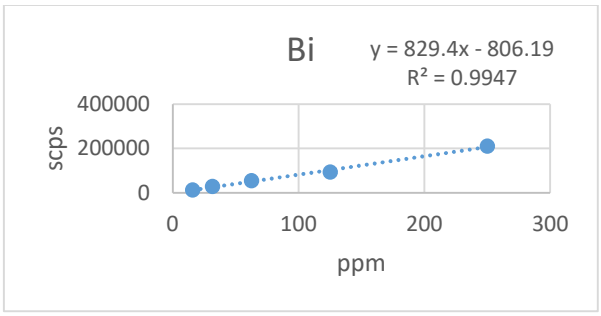

Figure 14 Rayleigh to Compton corrected linear regressions for nickel and bismuth peak heights.

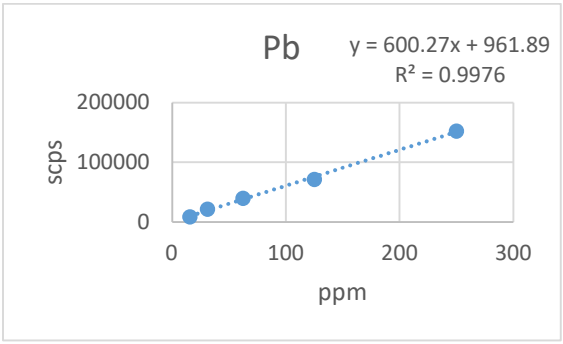

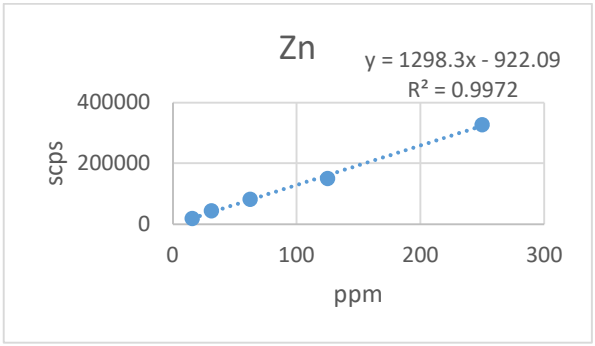

Figure 15 Rayleigh to Compton corrected linear regressions for lead and zinc peak heights.

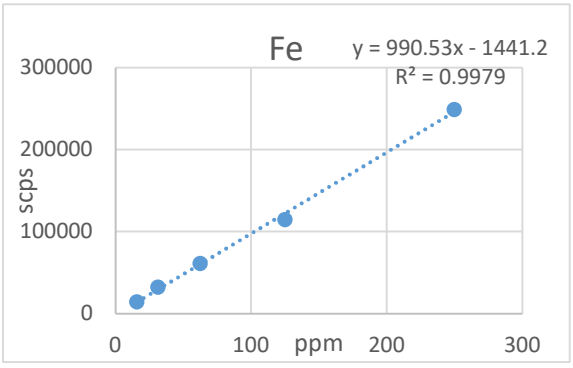

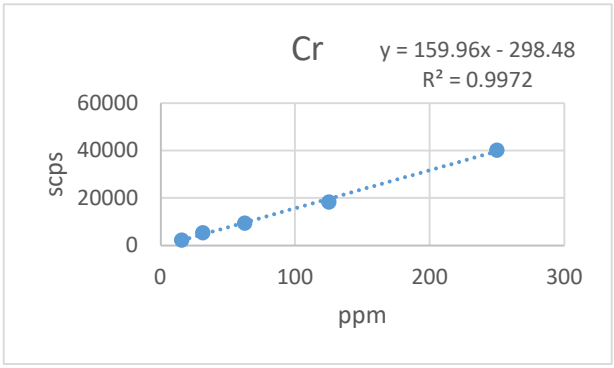

Figure 16 Rayleigh to Compton corrected linear regressions for iron and chromium peak heights.

After the trials with all the methods, this approach was chosen in the determination of the unknown since it gave better results compared to the other two methods.

Calculation of background corrected peak areas of the elements.

The peak area is calculated by taking the sum of all the spectrum signals and subtracting the average which is responsible for the background interference. This was done for all the curves and results recorded in the table below. Also, the regressions were made and recorded.

The table of Background Corrected Peak areas.

	ppm	250	125	62.5	31.25	15.625
Analyte						
Mn		142128.5	56496.5	30523.5	15223.5	7831.5
Cr	Background	89236	35093	18149	9265	4216
Co	corrected	367799.5	148373	78589	41338.5	18490
Fe	Peak Areas	183325.5	75179.5	39462	21897.5	10522.5
Zn		771381	322092	170299	91191	40166
Ni		441773	181509	94653	50772	23327

Table 6 Background corrected Peak areas.

Background Corrected Peak Areas Curves for Mn, Co, Ni, Fe, Cr and Zn

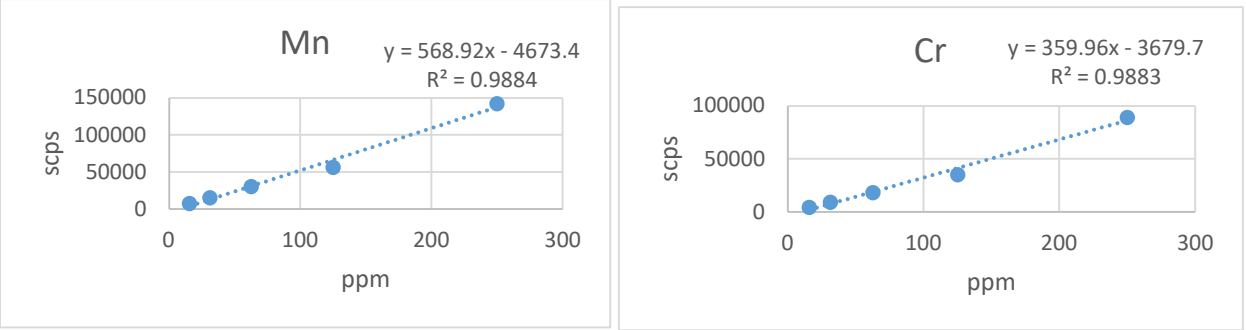

Figure 17 Background corrected peak area linear regression for manganese and chromium.

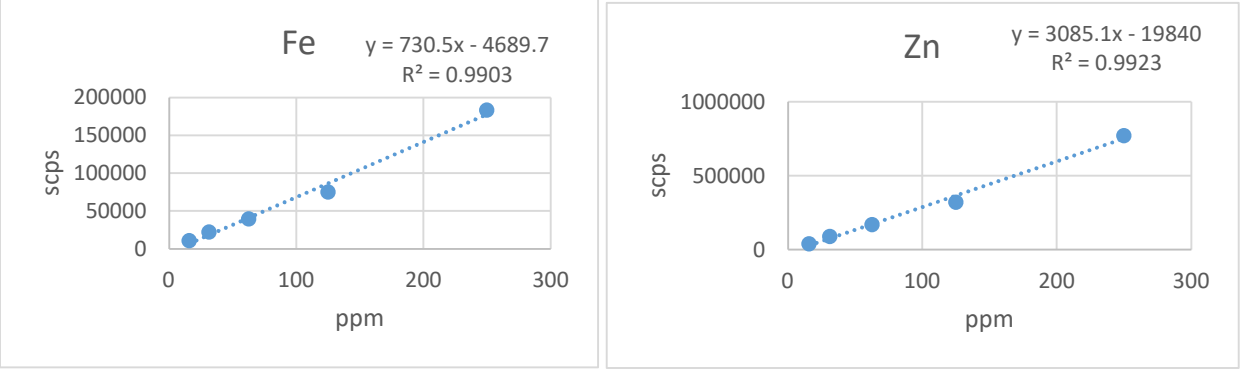

Figure 18 Background corrected peak area linear regressions for iron and zinc.

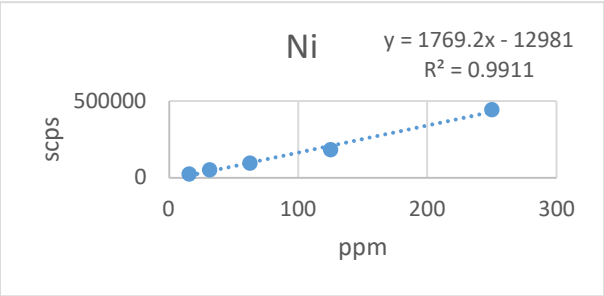

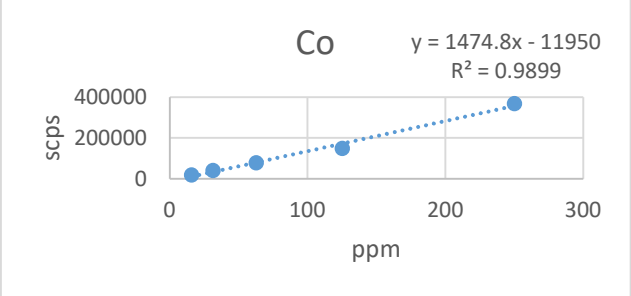

Figure 19 Background corrected peak area linear regression for nickel and cobalt.

Compton and Rayleigh peak areas and the Rayleigh to Compton peak area ratios

Concentration (ppm)	250	125	62.5	31.25	15.625
Compton (C)	2884514	4037626	4392960	4665973	4758923
Rayleigh (R)	486988	597967	622603	668779	681296
R/C	0.168828	0.14809866	0.14172744	0.143331	0.1431618

Table 7 Compton and Rayleigh peak areas and the Rayleigh to Compton peak areas

Calculation of Compton corrected peak areas.

The Compton correction was done by dividing the background corrected peak area with background corrected Compton peak areas. The results, as in peak heights, did not improve, as shown in the table below with corresponding regression coefficients.

The table of Compton Corrected Peak Areas

	ppm	250	125	62.5	31.25	15.625
Analyte						
Mn		1.38554	0.3917	0.19345	0.0971	0.0504
Cr	Compton	0.86992	0.243313	0.115025	0.059095	0.027134
Co	corrected	3.5855	1.0287	0.49808	0.26367	0.119
Fe	Peak Areas	1.787155	0.521249	0.250103	0.13967	0.067722
Zn		7.519835	2.23319	1.079327	0.581653	0.258508
Ni		4.30664	1.25847	0.59989	0.323844	0.150132

Table 8 Compton corrected Peak areas.

Compton Corrected Peak Area Curves for Mn, Co, Ni, Fe, Cr, and Zn

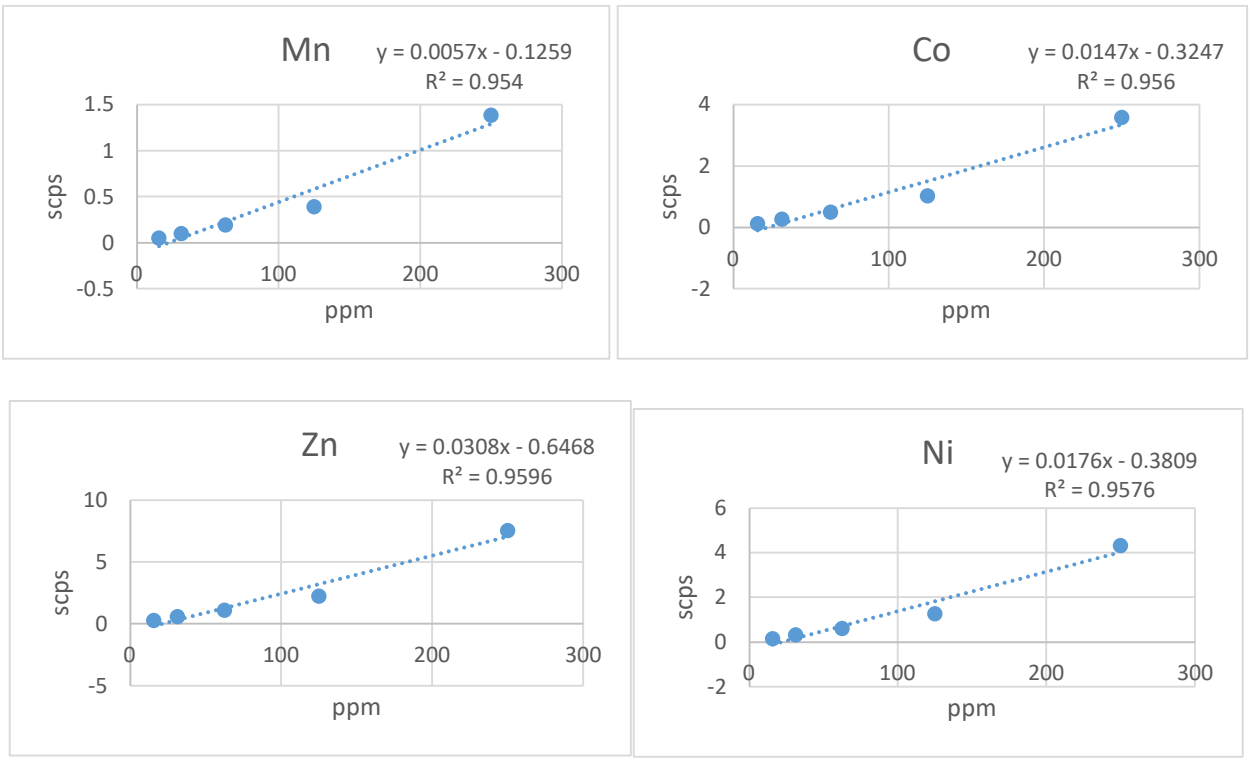

Figure 20 Compton corrected Peak areas linear regressions for Mn, Co, Ni and Zn

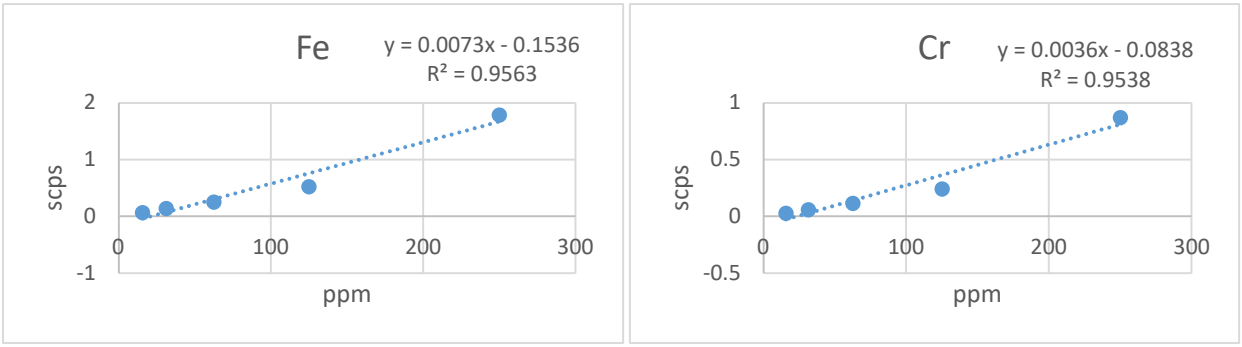

Figure 21 Compton corrected Peak areas linear regressions for Fe and Cr

Rayleigh to Compton corrected peak areas.

The data were further corrected by dividing the background corrected peak areas with ratios of Rayleigh to Compton peak areas, and this improved the regression data. The data and their corresponding regression data were recorded below.

The Table of Rayleigh to Compton Corrected Peak Areas

	ppm	250	125	62.5	31.25	15.625
Analyte						
Mn		841853.8394	381478.8061	215367.6098	106212.1942	54703.83859
Cr	R/C	528561.613	236956.9043	128055.6539	64640.58717	29456.1875
Co	corrected	2178545.62	1001852.414	554508.0049	288412.8346	129154.565
Fe	Peak Areas	1085871.419	507631.1967	278435.8484	152798.1299	73500.7523
Zn		4569034.757	2174847.497	1201595.188	636226.6362	280563.6699
Ni		2616704.575	1225595.154	667852.3227	354229.0223	162941.5109

Table 9 Rayleigh to Compton corrected peak areas.

The curves below are the regressions with their respective correlation coefficients of the Rayleigh to Compton corrected peak areas. They gave better results but not as peak heights. This is because the interference causes the peaks to be asymmetrical, which gives much error in the accuracy. (13)

Rayleigh to Compton Corrected Peak Area Curves for Mn, Co, Ni, Fe, Cr and Zn

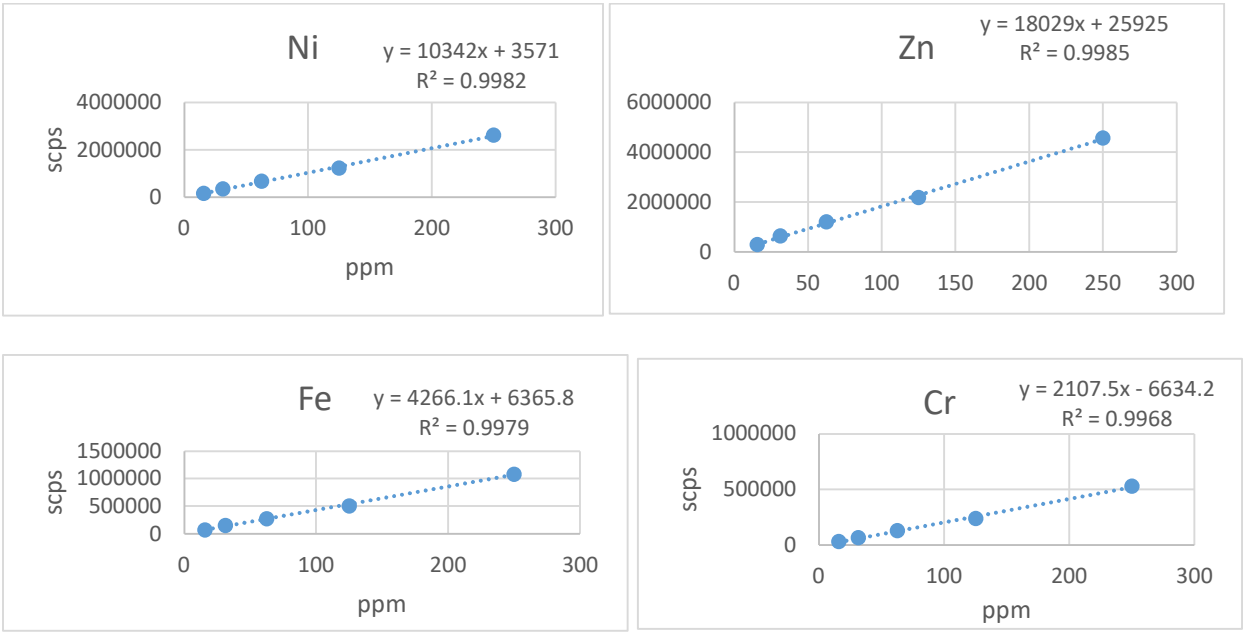

Figure 22 Rayleigh to Compton corrected Peak area linear regressions for Ni, Zn, Fe and Cr

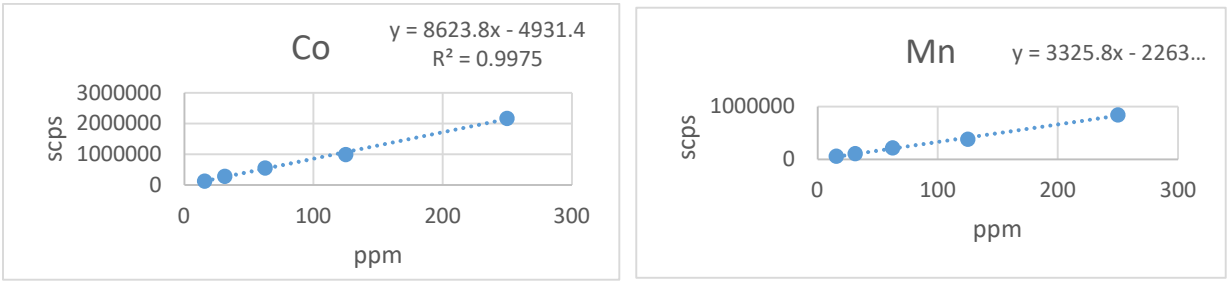

Figure 23 Rayleigh to Compton Peak area linear regressions for Co and Mn

Data of background corrected peak heights and peak areas and Rayleigh to Compton Corrected peak heights and peaks areas.

The data for both peak heights and peak areas were tabulated to analyze the unknowns. Corrections based on Compton corrections were omitted because there was no improvement with only Compton corrections.

The correction based on Rayleigh to Compton ratios gave better results compared to the other two methods used above (background correction alone as well as background corrected divided by Compton peaks.) The approach, which was also one of the methods used by P M S Carvalho et al is also the method they recommended in their trace metal analysis in biological samples. (13)

The Table Background and Rayleigh to Compton Corrected Peak Heights and Areas Regression Parameters

Element	**Peak**	**Height**	**Peak**	**Area**
	BK Corrected	**R/C Corrected**	**BK Corrected**	**R/C Corrected**
Mn		y = 260.87x - 1509.2		y = 3325.8x - 2263
	R^2 = 0.9859	R^2 = 0.993	R^2 = 0.9884	R^2 = 0.9967
Cr		y = 159.96x - 298.48		y = 2107.5x - 6634.2
	R^2 = 0.9918	R^2 = 0.9972	R^2 = 0.9883	R^2 = 0.9968
Co		y = 543.07x - 1916.8		y = 8623.8x - 4931.4
	R^2 = 0.9925	R^2 = 0.9976	R^2 = 0.9899	R^2 = 0.9975
Fe		y = 990.53x - 1441.2		y = 4266.1x + 6365.8
	R^2 = 0.9992	R^2 = 0.9979	R^2 = 0.9903	R^2 = 0.9979
Pb		y = 1595.8x + 123.59		
	R^2 = 0.9934	R^2 = 0.9976		
Bi		y = 829.4x - 806.19		
	R^2 = 0.989	R^2 = 0.9947		
Zn		y = 1298.3x - 922.09		y = 18029x + 25925
	R^2 = 0.9923	R^2 = 0.9972	R^2 = 0.9911	R^2 = 0.9985
Ni		y = 708.84x + 1895.7		y = 10342x + 3571
	R^2 = 0.9934	R^2 = 0.9982	R^2 = 0.9911	R^2 = 0.9982

Table 10 Regression Coefficients of R/C and Background Corrected Peak Heights and Areas

The corrections were further investigated by dividing the background corrected peak areas with Rayleigh(R) to Compton (C) ratios, improving the regression data. The data were tabulated and recorded and are shown in the table below. The regressions were also made and recorded. The correction based on Rayleigh to Compton ratios gave the

better results comparing to the other two methods used (background corrected alone as well as Compton corrected) The approach which was also one of the methods used by P M S Carvalho et al is also the method they recommended in their trace metal analysis in biological samples. (13). The correlation coefficients lead, manganese and iron resemble the ones provided in the literature (25). Other elements that were analyzed also provided the correlation coefficient like iron lead and manganese.

Limits of detections

When measurements are taken to develop a calibration curve, it is expected that all the signals align on the regression. However, this is often not the case due to errors during the analysis. These errors cause the deviation from linearity. The vertical deviation along the y axis causes uncertainty during the quantitative analysis. This makes it difficult to differentiate between the smallest detectable signal and the background. This drawback is resolved by calculating the lowest quantifiable signal, also known as limit of detection. This is done by taking the average of standard deviation of all the residuals, dividing by the slope, and subsequently multiplying by a factor of three, as illustrated below.

The figure of residuals

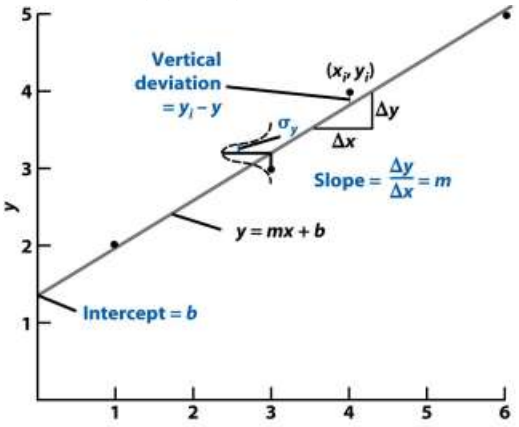

Figure 24 Graphical representation of residuals

The limit of detections is calculated by applying the formula as:

$$LOD = \frac{3}{b} * (y)$$

b is the gradient of the curve which is also called sensitivity. It is measured in counts per seconds per unit concentrations of the analytes. These counts are provided by the instrument and y is the standard deviation of residual. It is measured in counts per seconds (25).

The limit of quantification is calculated by applying a factor of 3.3 to the limit of detection.

The limits of detections and quantifications are recorded in the below table.

The table of limits of detection and limits of quantification

Analyte	LOD (ppm)	LOQ (ppm)
Mn	1	3
Fe	1	4
Co	1	4
Ni	1	5
Zn	4	13
Cr	0.05	0.2

Table 11Limits of detection and limits of quantifications

Determinations of the concentrations of the analytes from the selected samples

The samples of teas pharmaceutical products, coffee as well as food spices were run, spectra developed from the data that were later used to signal determinations and quantifications of the unknowns from the samples using the calibration curves. The spectra to the various samples are provided below to which the unknown elements were quantified.

Teas and coffees

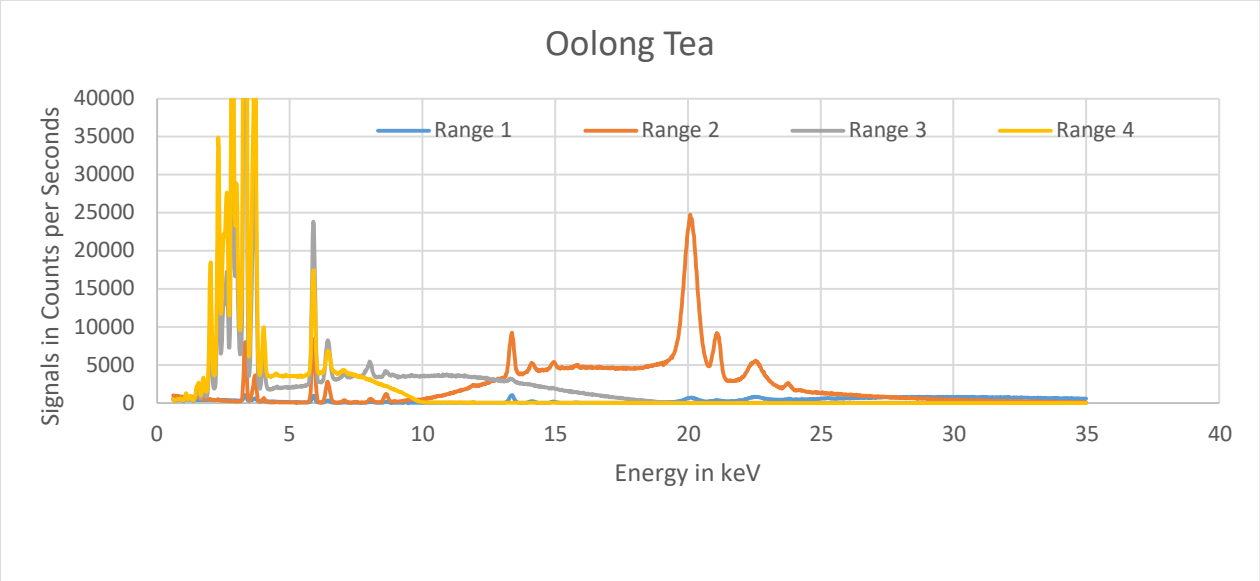

Figure 25 Oolong Tea Graph

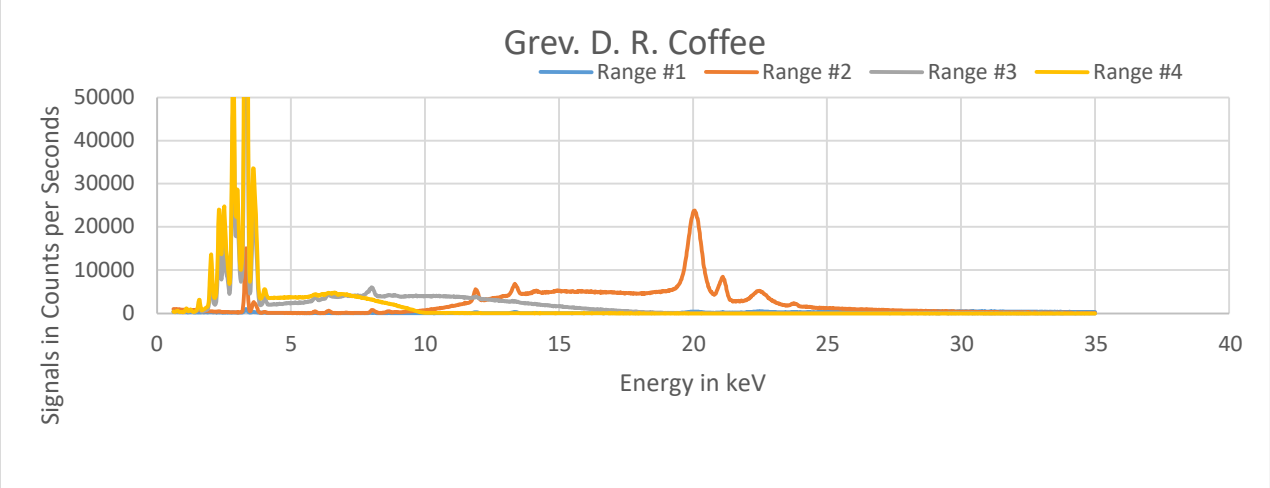

Figure 26 Grev. D. R. Coffee

Pharmaceuticals

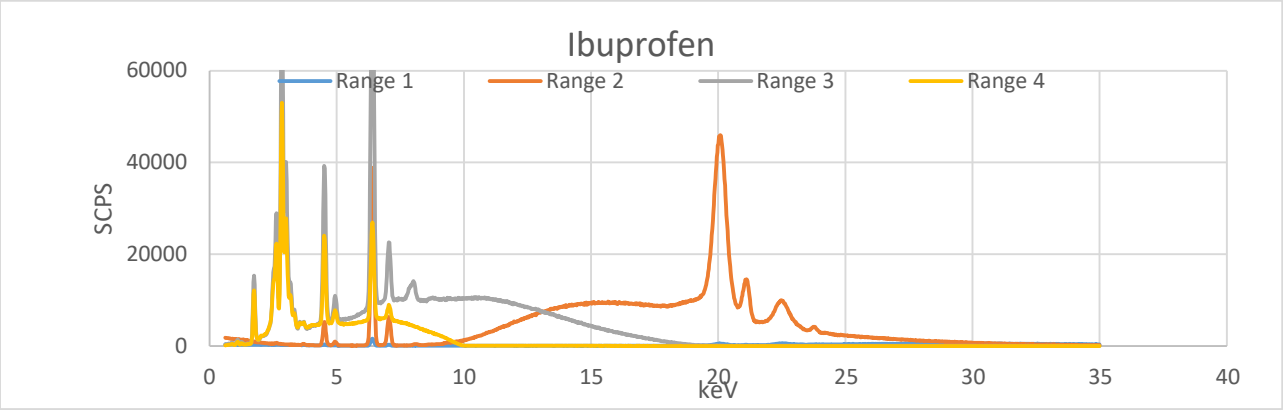

Figure 27 Ibuprofen

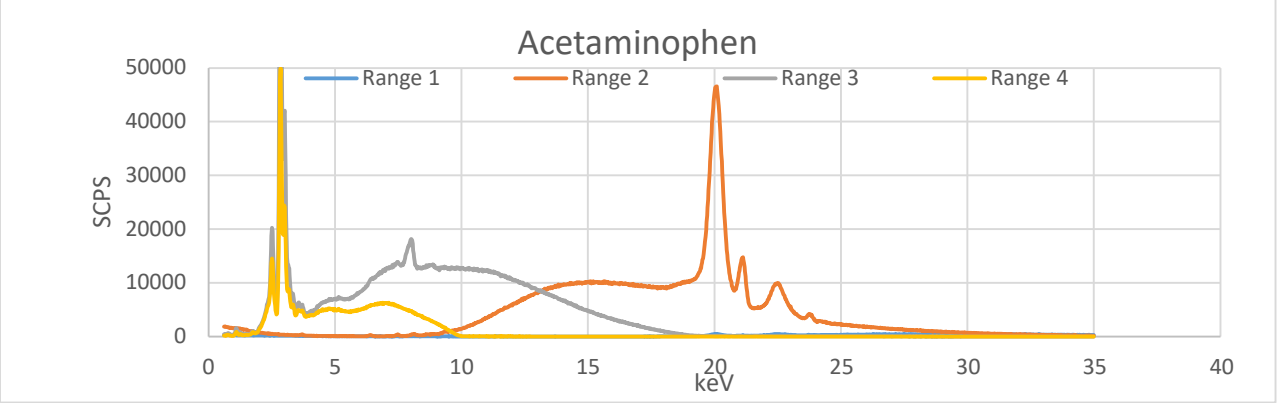

Figure 28 Acetaminophen

Food Spices

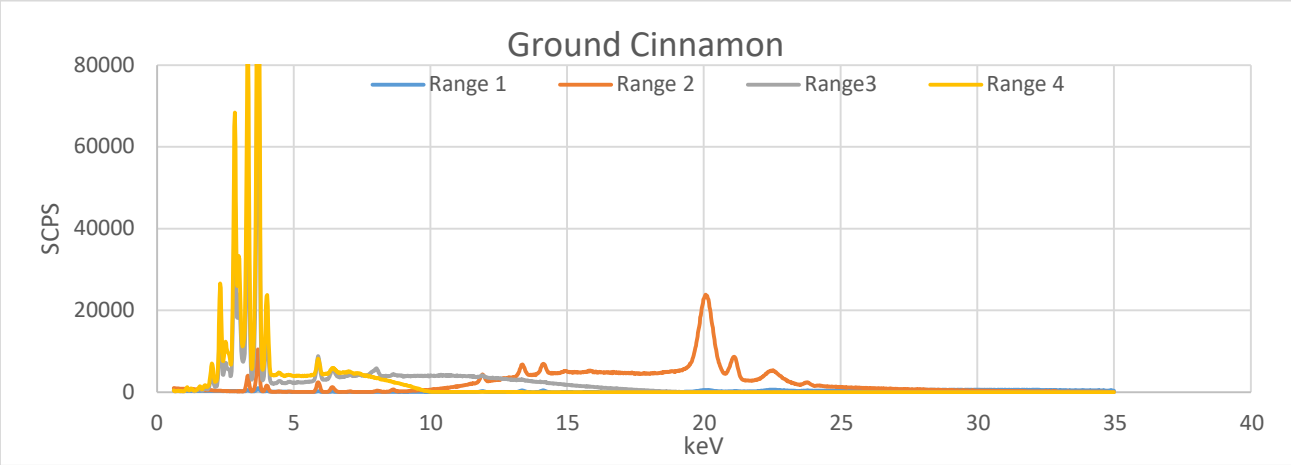

Figure 29 Ground Cinnamon

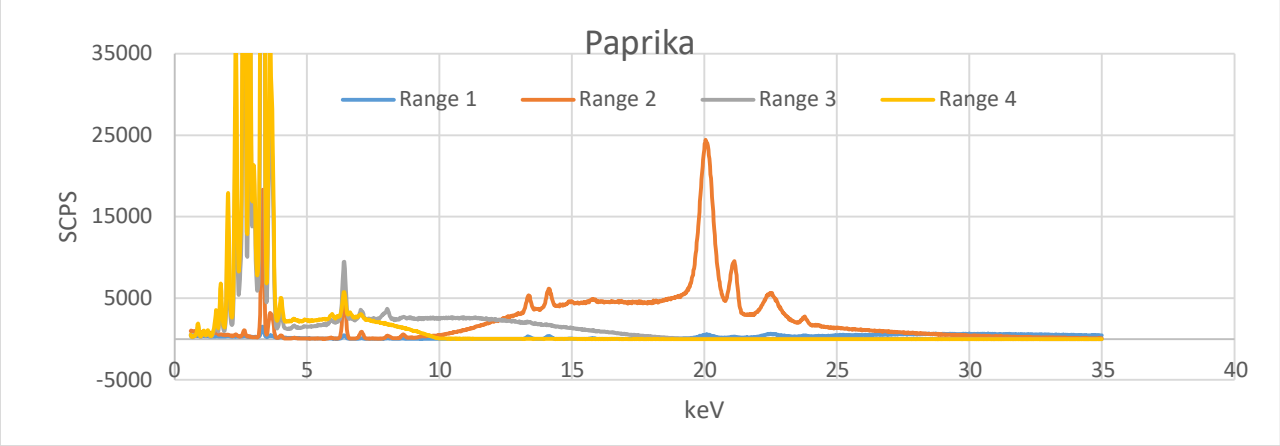

Figure 30 Paprika

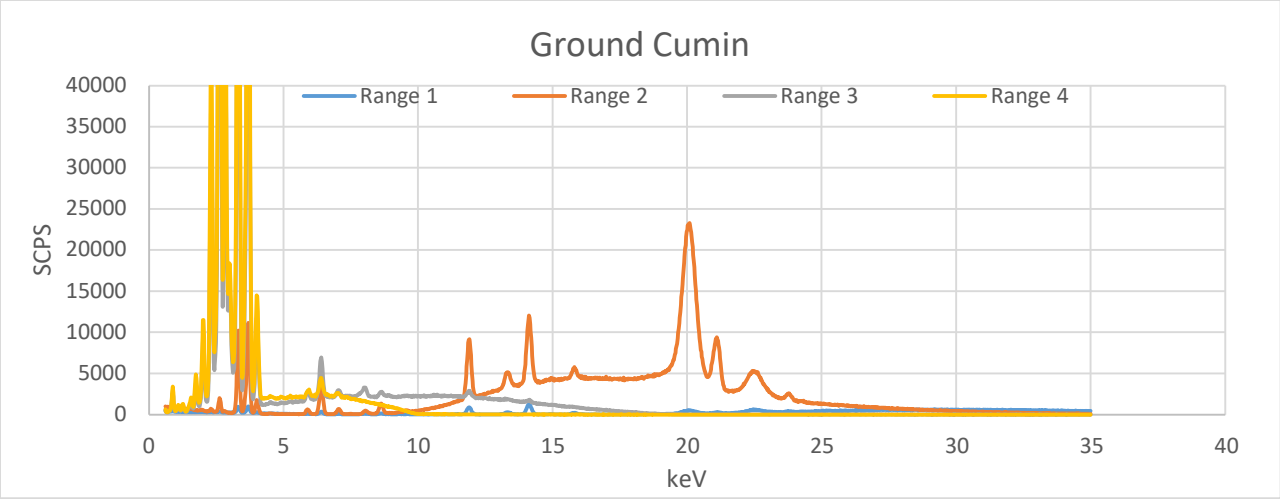

Figure 31Ground Cumin

From the spectra of all the samples as well as the solution standard, four ranges were recorded. Of the four ranges, range two gave a remarkably high number of counts per seconds of the Compton and Rayleigh signals. For this reason, range two was used for the analysis of all the samples since in the analysis the Compton and Rayleigh peaks were used for background corrections.

Compton and Rayleigh ratios of the samples

The table below shows all the data calculated to realize the ratios of Rayleigh to Compton peak areas and peak heights that were used in the corrections of background corrected peak heights and peak area for all the unknown samples. The analysis was carried out in parts per million concentrations.

The table of Compton and Rayleigh ratios of the Samples

Compton (C)	Oolong Tea	G Cumin	Cinnamon	Paprika	Ibuprofen	Acetaminophen	Grev.D.R. coffee	E. G. Black Tea	Steep Lemon Ginger Herbal Tea
P. H (20.089)	24780	23310	23700	24080	45970	46560	23390	23700	24230
Average BK	5290	5000	5154	5293	9508	9924	5086	5248	5182
Corrected P.H-Compton	19490	18310	185500	18790	36460	36630	1831	18450	19050
Corrected P Area-Compton	566200	541300	555400	563300	1065000	1079000	550000	548800	571600
Rayleigh, R									
P. H (21.109)	9100	9375	8695	9453	14250	14630	8420	8653	8880
Average BK	3926	3756	3758	3878	7015	6966	3607	3731	3845
Corrected P.H (R)	5174	5619	4938	5576	7234	7659	4813	4922	5035
Corrected P. A (R)	78280	82150	72640	84450	108200	113500	68620	74760	74130
H (R/C)	0.265	0.307	0.266	0.297	0.198	0.209	0.263	0.267	0.264
A(R/C)	0.138	0.152	0.131	0.150	0.102	0.105	0.125	0.136	0.130

Table 12 Compton and Rayleigh Ratios of the Samples

Manganese (Mn)

This analyte is produced at 5.900 (K alpha) keV, from the literature (17). In our laboratory, it was produced at 5.909 keV, a deviation of 0.9%, which is within the allowed variance in energy.

The spectra above were used to quantify the analyte and the results recorded in the table below. Using the calibration data for manganese, the concentrations were also determined and recorded below. The analysis was carried out in parts per million concentrations.

The table of Manganese Concentrations in the Samples

	Oolong Tea	Ground Cumin	G Cinnamon	Paprika	Ibuprofen	Acetaminophen	Grev.D.R. coffee	Early Grey Black Tea	Steep Lemon Ginger Herbal Tea
P. height (5.909)	8406	593	2398	147	100	63	415	9559	1806
Average background	117.5	40.00	61.00	42.00	95.50	59.00	39.00	118.0	53.00
Corrected P. Height	**8289**	**553.0**	**2337**	**105.0**	**4.500**	**4.000**	**376.0**	**9441**	**1753**
Corrected P Area	**60350**	**4345**	**17920**	**879.0**	**14.00**	**95.00**	**2533**	**67820**	**12680**
H (R/C)	0.265	0.307	0.266	0.297	0.198	0.209	0.263	0.267	0.264
A (R/C)	0.138	0.152	0.131	0.150	0.102	0.105	0.125	0.136	0.130
P. Height/(R/C)	**31230**	**1802**	**8778**	**353.7**	**22.68**	**19.13**	**1430**	**35390**	**6631**
P. Area/(R/C)	**436500**	**28630**	**136900**	**5863**	**137.7**	**903.2**	**20300**	**497900**	**97730**
Mass ratio									
Peak height	a	b							
y = 260.87x - 1509.2	260.9	-1509							
ppm	125.5	12.69	39.43	7.141	5.872	5.859	11.27	141.5	31.20
Peak area									
y = 3325.8x - 2263	3326	-2263							
ppm	131.9	9.289	41.87	2.443	0.7212	0.952	6.785	150.4	30.07

Table 13 Manganese, Mn

In this analysis, there is a difference in concentration between measurements based on peak height and those based on peak areas. One of the main reasons that causes this difference is the symmetry of the signals. Asymmetrical signal will give a very wide disparity between the concentration based on peak height and peak areas. A non-normal distributed peak will be related to a large error on the peak area (13). When peak height is so small, as in the case of paprika, acetaminophen, Ibuprofen, Acetaminophen, Grev D.R. coffee as well as ground cumin in this analysis, sometimes it becomes smaller than the amount necessary to be reported as signal and subsequently cannot be quantified, it can give the exceedingly small peak height but large enough peak area that can be quantified. However, Ibuprofen and Acetaminophen also gave very strange signals that appeared like background noise. In General, peak heights give remarkably high concentration and this can be attributed to some incomplete background subtraction from the signals. This makes concentrations due to peak areas more reliable compared to peak heights. This is seen for all the samples in this analyte. In this analysis, the analyte was detectable in all the samples and quantifiable.

Iron (Fe)

This analyte is produced at 6.405 (K alpha) kiloelectronvolts, from the literature (17). In our laboratory, it was produced at 6.409, a deviation of 0.4%, which is within the allowed variance in energy.

The spectra above were used to quantify the analyte and the results recorded in the table below. Using the calibration data for manganese, the concentrations were also determined and recorded below. The analysis was carried out in parts per million concentrations.

The table of Iron Concentrations in the Samples

	Oolong Tea	Ground Cumin	G Cinnamon	Paprika	Ibuprofen	Acetaminophen	Grev.D.R. coffee	Early Grey Black Tea	Steep Lemon Ginger Herbal Tea
P. height (6.409)	2721	4008	1235	5286	38820	261.0	562.0	3011	3597
Average background	258.0	98.00	110.0	98.50	550.0	59.50	38.00	300.0	108.0
Corrected P. Height	**2463**	**3910**	**1125**	**5188**	**38270**	**201.5**	**524.0**	**2711**	**3489**
Corrected P Area	**21470**	**29310**	**9391**	**39070**	**288100**	**1540**	**4382**	**23530**	**26480**
H (R/C)	0.265	0.307	0.266	0.297	0.198	0.209	0.263	0.267	0.264
A (R/C)	0.138	0.152	0.131	0.150	0.102	0.105	0.125	0.136	0.130
P. Height/(R/C)	**9280**	**12740**	**4226**	**17470**	**192900**	**963.7**	**1993**	**10160**	**13200**
P. area/(R/C)	**155300**	**193100**	**71800**	**260600**	**283500**	**14640**	**35120**	**172700**	**204200**
Mass ratio									
Peak height	a	b							
y = 990.53x - 1441.2	990.5	-1441							
ppm	10.82	14.32	5.721	19.10	196.2	2.428	3.467	11.72	14.78
Peak area									
y = 4266.1x + 6365.8	4266	6366							
ppm	34.91	43.78	15.34	59.60	663.0	1.940	6.740	39.00	46.37

Table 14 Iron, Fe

In this analysis, there is a difference in concentration between measurements based on peak height and those based on peak areas. One of the main reasons that causes this difference is the symmetry of the signals. Asymmetrical signal will give a very wide disparity between the concentration based on peak height and peak areas. A non-normal distributed peak will be related to a large error on the peak area (13). In this analysis Acetaminophen and Grev. D. R. coffee has a non-normal distributed signal. This makes the concentration based on peak areas so much unreliable compared to concentrations based on peak heights. The samples that distributed peaks are Ibuprofen, Paprika, Ground cumin and steep lemon herbal tea. The samples that gave a tailing signal are Oolong tea and early grey black tea. In General, peak heights give exceedingly high concentration and this can be attributed to some incomplete background

subtraction from the signals. This makes concentration due to peak areas more reliable compared to peak heights. This is seen for all the samples in this analyte. In this analysis iron was detectable from all the samples, however, it was below the limit that could be quantified in Acetaminophen and Grev.D. R Coffee.

Cobalt (Co)

This analyte is produced at 6.931(K alpha) kiloelectronvolts, from the literature (17). In our laboratory, it was produced at 7.049, a deviation of 11.8%, which is within the allowed variance in energy. The spectra above were used to quantify the analyte and the results recorded in the table below. Using the calibration data for manganese, the concentrations were also determined and recorded below. The analysis was carried out in parts per million concentrations.

The table of Cobalt Concentrations in the Samples

	Oolong Tea	Ground Cumin	G Cinnamon	Paprika	Ibuprofen	Acetaminophen	Grev.D.R. coffee	Early Grey Black Tea	Steep Lemon Ginger Herbal Tea
P. height (7.049)	334.0	658.0	210.0	897.0	6322	104.0	124.0	381.0	556.0
Average background	40.00	41.00	38.50	44.50	162.0	67.00	43.00	49.00	52.00
Corrected P. Height	**294.0**	**617.0**	**171.5**	**852.5**	**6160**	**37.00**	**81.00**	**332.0**	**504.0**
Corrected P Area	**2501**	**5178**	**1275**	**6995**	**49730**	**166.0**	**628.0**	**2832**	**4146**
H (R/C)	0.265	0.307	0.266	0.297	0.198	0.209	0.263	0.267	0.264
A (R/C)	0.138	0.152	0.131	0.150	0.102	0.105	0.125	0.136	0.130
P. Height/(R/C)	**1107**	**2010**	**644.2**	**2872**	**31040**	**177.0**	**308.1**	**1244**	**1906**
P. area/(R/C)	**18090**	**34120**	**9744**	**46660**	**489200**	**1578**	**5033**	**20790**	**31970**
Mass ratio									
Peak height	a	b							
y = 543.07x - 1916.8	543.1	-1917							
ppm	5.569	7.232	4.716	8.818	60.69	3.855	4.097	5.821	7.040
Peak area									
y = 8623.8x - 4931.4	8624	-4931							
ppm	2.670	4.528	1.702	5.982	57.30	0.755	1.155	2.983	4.279

Table 15 Cobalt (Co)

In this analysis, there is a difference in concentration between measurements based on peak height and those based on peak areas. One of the main reasons that causes this difference is the symmetry of the signals. Asymmetrical signal will give a very wide disparity between the concentration based on peak height and peak areas. A non-normal distributed peak will be related to a large error on the peak area (13). The oolong tea, ground cumin and ground cinnamon are very asymmetrical. Ibuprofen and paprika

have very normal distributed signals and this reduce errors in both analyses. Acetaminophen has a signal that resembles a horizontal background peak. In General, peak heights give extremely high concentration and this can be attributed to some incomplete background subtraction from the signals. This makes concentrations due to peak areas more reliable compared to peak heights. This is seen for all the samples in this analyte. In this analysis, cobalt was detectable in all the samples. However, it was below the limit of quantification in Acetaminophen.

Nickel (Ni)

This analyte is produced at 7.480 (K alpha) kiloelectronvolts, from the literature (17). In our laboratory, it was produced at 7.449, a deviation of 3.1%, which is within the allowed variance in energy.

The spectra above were used to quantify the analyte and the results recorded in the table below. Using the calibration data for manganese, the concentrations were also determined and recorded below. The analysis was carried out in parts per million concentrations.

The table of Nickel Concentrations in the Samples

	Oolong Tea	Ground Cumin	G Cinnamon	Paprika	Ibuprofen	Acetaminophen	Grev.D.R. coffee	Early Grey Black Tea	Steep Lemon Ginger Herbal Tea
P. height (7.449)	165.0	74.00	53.00	55.00	92.00	352.0	59.00	188.0	91.00
Average background	34.00	39.50	44.50	45.50	78.50	87.50	38.50	53.00	38.50
Corrected P. Height	**131.0**	**34.50**	**8.500**	**9.500**	**13.50**	**264.5**	**20.50**	**135.0**	**52.50**
Corrected P Area	**991.0**	**267.5**	**95.50**	**153.5**	**81.50**	**2171**	**152.5**	**942.0**	**515.5**
H (R/C)	0.265	0.307	0.266	0.297	0.198	0.209	0.263	0.267	0.264
A (R/C)	0.138	0.152	0.131	0.150	0.102	0.105	0.125	0.136	0.130
P. Height*R/C	**493.6**	**112.4**	**31.93**	**32.00**	**68.04**	**1265**	**77.98**	**506.1**	**198.6**
P. area*R/C	**7168**	**1762**	**730.2**	**1023**	**801.8**	**20640**	**1222**	**6915**	**3975**
Mass ratio									
Peak height	a	b							
y = 708.84x + 1895.7	708.8	1895							
ppm	n.d	n.d	n.d	n.d	n.d	n.d	n.d	n.d	n.d
Peak area									
y = 10342x + 3571	10340	3571							
ppm	0.348	-0.175	-0.275	-0.229	-0.268	1.650	-0.227	0.323	0.039

Table 16 Nickel Ni

In this analysis, there is a difference in concentration between measurements based on peak height and those based on peak areas. One of the main reasons that causes this difference is the symmetry of the

signals. Asymmetrical signal will give a very wide disparity between the concentration based on peak height and peak areas. A non-normal distributed peak will be related to a large error on the peak area (13). The signals for all the signals were very asymmetrical. This makes it hard to subtract the errors and measure absolute peak heights. In General, the peak areas give remarkably high concentration, and this can be attributed to asymmetrical signals subtraction from the signals this makes concentrations due to peak height more reliable compared to peak areas. This is seen for all the samples in this analyte. The concentration of Nickel in the samples is low compared to the concentrations detailed in the literature by Shimazu and the core authors. However, the method will provide a suitable alternative for other methods such as ICP-MS in the analysis of the element (16). Nickel was not detected in Acetaminophen. The analyte was also below the quantifiable limit for all the samples.

Zinc (Zn)

This analyte is produced at 8.637(K alpha) kiloelectronvolts, from the literature (17). In our laboratory, it was produced at 8.629, a deviation of 0.8%, which is within the allowed variance in energy.

The spectra above were used to quantify the analyte and the results recorded in the table below. Using the calibration data for manganese, the concentrations were also determined and recorded below. The analysis was carried out in parts per million concentrations.

The table of Zinc Concentrations in the Samples

	Oolong Tea	Ground Cumin	G Cinnamon	Paprika	Ibuprofen	Acetaminophen	Grev.D.R. coffee	Early Grey Black Tea	Steep Lemon Ginger Herbal Tea
P. height (8.629)	1184	1333	626.0	582.0	330.0	399.0	485.0	1267	680.0
Average background	172.5	199.0	167.0	136.0	244.0	290.0	166.0	230.5	161.0
Corrected P. Height	**1012**	**1134**	**459.0**	**446.0**	**86.00**	**109.0**	**319.0**	**1037**	**519.0**
Corrected P Area	**8315**	**8918**	**3768**	**3387**	**674.0**	**986.0**	**2321**	**8233**	**4327**
H (R/C)	0.265	0.307	0.266	0.297	0.198	0.209	0.263	0.267	0.264
A (R/C)	0.138	0.152	0.131	0.150	0.102	0.105	0.125	0.136	0.130
P. Height/(R/C)	**3811**	**3695**	**1724**	**1502**	**433.4**	**521.3**	**1213**	**3886**	**1963**
P. area/(R/C)	**60140**	**58760**	**28810**	**22590**	**6631**	**9374**	**18600**	**60430**	**33360**
Mass ratio									
Peak height	a	b							
y = 1298.3x - 922.09	1298	-922.1							
ppm	n.d	n.d	n.d	n.d	n.d	n.d	n.d	n.d	n.d
Peak area									
y = 18029x + 25925	18030	25930							
ppm	1.898	1.821	0.160	-0.185	-1.070	-0.918	-0.406	1.914	0.413

Table 17 The Concentrations of Zinc in samples.

In this analysis, there is a difference in concentration between measurements based on peak height and those based on peak areas. One of the main reasons that causes this difference is the symmetry of the signals. Asymmetrical signal will give a very wide disparity between the concentration based on peak height and peak areas. A non-normal distributed peak will be related to a large error on the peak area (13). The signals for all the have very asymmetrical signals. This introduces errors in terms of concentrations in terms of peak heights. In General, peak heights give extremely high concentration and this can be attributed to some incomplete background subtraction from the signals. This makes concentrations due to peak areas more reliable compared to peak heights. This is seen for all the samples in this analyte. The analyte was not detected in all the samples.

Standard Reference Material (Tomato leaves)

The material was analyzed the same way the other analytes were analyzed, and the concentration calculated and tabulated below.

The table of peak height, R/C corrected concentrations in ppm

Element	**Height**	y=ax+b			Certified value
	R/C Corrected	a	b	ppm	ppm
Mn	y = 260.87x - 1509.2	260.9	-1509	20.45	238+/-7
Co	y = 543.07x - 1916.8	543.1	-1916	5.962	
Fe	y = 990.53x - 1441.2	990.5	-1441	10.30	690+/-25
Zn	y = 1298.3x - 922.09	1298	-922.1	2.461	62+/-6
Ni	y = 708.84x + 1895.7	708.8	1896		

Table 18 The table of Standard reference materials

From the table, the values do not agree with the certified values, and this could be due to many factors ranging from instrumental malfunctions to human errors. This makes the method not a sensitive method but an immensely powerful tool for fastening the production chain by providing random screening of the selected toxic elements in the products and the ones that are highly concentrated are stopped from the conveyor as the rest of the products that have the acceptable concentrations are allowed in the production chain. The uncertainties on the certified are provided as negatives or positives.

ICP-MS DATA ANALYSIS

The calibration curves were generated by the instrument, which was used to quantify the samples in ppb. The results were further divided by a factor of 1000 to convert them to parts per ppm, which is the concentrations used for the analysis of the samples in XRF. This enables side by side comparison of the sample concentrations of both instruments and with the data of the certificated provided for by the USP for the SRM (26).

The figure of Mn ICP-MS instrument

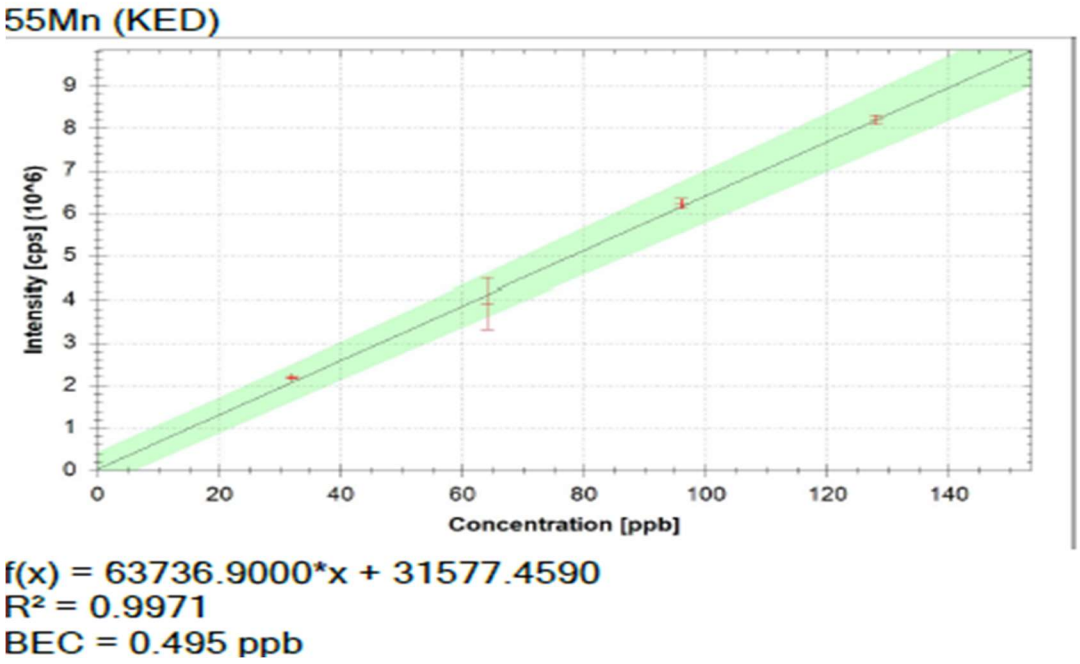

Figure 32 Manganese ICP calibration curve for SRM

The figure above is an example of the calibration curves generated by the instrument for manganese 55 isotope. It provides a background error correction of 0.495 ppb. The curve gave a linear relationship with concentrations and provides a powerful tool for compression with the XRF method results developed.

ICP-MS table generated from the elements in ppb.

Sample Line	52Cr (KED)	55Mn (KED)	56Fe (KED)	57Fe (KED)	59Co (KED)	60Ni (KED)	64Zn (KED)	66Zn (KED)	206Pb (KED)
SRM (Tomato Leaves)	**1603.1**	**118244.4**	282622.5	72267.8	451.3	789.1	8800.6	5693.2	238.2
Acetaminophen	**901.1**	**314.2**	27469.1	13843.4	68.0	8352.7	8412.8	2631.6	215.8
Paprika	**3639.2**	**13293.1**	662647.8	163954.3	371.0	4593.8	17242.7	5326.0	251.7
Centrum	**25060.5**	**768752.9**	33211.3	28376.7	1480.2	1267.7	2659360.2	852130.8	-61.4
Tag lass tea	**3941.6**	**970041.9**	210436.1	104432.8	365.8	7843.6	29674.6	9889.6	3322.4
Oolong Tea	**1416.6**	**788048.5**	350474.6	172491.0	442.3	9813.4	40059.6	13405.6	1483.2
G. Cinnamon	**1392.8**	**210481.2**	138583.9	70196.9	323.0	8268.1	26379.4	8717.2	75.3
G. Cumin	**1809.4**	**54712.2**	425250.9	211635.4	393.4	1760.5	31067.7	10176.2	438.9
Ibuprofen	**942.7**	**1487.0**	2430701.6	1215860.5	285.8	11828.9	9890.7	3081.3	299.6
Green Tea	**1658.5**	**777480.1**	220321.2	109694.7	606.9	4403.8	26105.3	8952.2	1234.3

Table 19 Concentrations of Analytes From ICP-MS in ppb

The conversion of ppb to ppm was done using the following operation and results tabulated below.

$$1ppb = \frac{1}{1000ppm}; concentration = ppm * (ppb * \frac{1}{1000ppb})$$

The table of Concentrations of Analytes in ppm

Sample Line	52Cr (KED)	55Mn (KED)	56Fe (KED)	57Fe (KED)	59Co (KED)	60Ni (KED)	64Zn (KED)	66Zn (KED)	206Pb (KED)
SRM (Tomato leaves)	**1.600**	**118.2**	**282.6**	**72.30**	**0.500**	**0.800**	**8.800**	**5.700**	**0.200**
Acetaminophen	**0.900**	**0.300**	**27.50**	**13.80**	**0.100**	**8.400**	**8.400**	**2.600**	**0.200**
Paprika	**3.600**	**13.30**	**662.6**	**164.0**	**0.400**	**4.600**	**17.20**	**5.300**	**0.300**
Centrum	**25.10**	**768.8**	**33.20**	**28.40**	**1.500**	**1.300**	**2659**	**852.1**	**-0.100**
Tag lass tea	**3.900**	**970.0**	**210.4**	**104.4**	**0.400**	**7.800**	**29.70**	**9.900**	**3.300**
Oolong Tea	**1.400**	**788.0**	**350.5**	**172.5**	**0.400**	**9.800**	**40.10**	**13.40**	**1.500**
G. Cinnamon	**1.400**	**210.5**	**138.6**	**70.20**	**0.300**	**8.300**	**26.40**	**8.700**	**0.100**
G. Cumin	**1.800**	**54.70**	**425.3**	**211.6**	**0.400**	**1.800**	**31.10**	**10.20**	**0.400**
Ibuprofen	**0.900**	**1.500**	**2431**	**1215.9**	**0.300**	**11.80**	**9.900**	**3.100**	**0.300**
Green Tea	**1.700**	**777.5**	**220.3**	**109.7**	**0.600**	**4.400**	**26.10**	**9.000**	**1.200**

Table 20 ICP-MS Analytes concentrations in ppm

Comparisons of ICP-MS, XRF and the Certified values of Mn

The values for both the ICP and XRF are in ppm. This is because the certified values are given in ppm, and it is only possible to compare values when the concentrations are given in the same units. The table below was generated for comparisons of the values to validate the method.

The table of comparisons of ICP-MS XRF and Certified Values of Mn, Fe and Zn

Analyte	ICP-MS	XRF	Certified values
	ppm	ppm	ppm
Mn	118	20.5	238+/-7
Fe	238	10.3	690+/-25
Zn	3.10	2.02	11+/-1

Table 21 Comparison of ICP-MS, XRF and Certified Values

From the table, the values do not agree with the certified values, and this could be due to many factors ranging from instrumental malfunctions to human errors. This makes the method not a sensitive method but a powerful tool for fastening the production chain by providing random screening of the selected toxic elements in the products and the ones that are highly concentrated are stopped from the conveyor as the rest of the products that have the acceptable concentrations are allowed in the production chain. The uncertainties on the certified are provided as negatives or positives.

CONCLUSIONS AND FUTURE DIRECTIONS

Our results indicate that XRF has potential to be a useful method for screening and provide approximate concentrations that can for example indicate if a material has trace element levels that are within an acceptable range. Standardizations and confirmations should be done with more sensitive methods like ICP-MS, when an exceptionally low detection limit is required. The use of XRF as a screening method has the potential to speed up the in-situ analysis and allow rapid identification of samples or materials that have trace metal concentrations that are likely to exceed or fall below an established guideline.

BIBLIOGRAPHY-LIST OF REFERENCES

References

1. *Elemental Analysis Using Atomic Absorption Spectroscopy.* **Mohammed, Abdul Moiz.** 2021, European Journal of Engineering and TechnologyResearch, pp. 2736-5769.

2. **Vickers, J.D Winefornder and T.J.** Atomic Fluoresence Spectromentry as a Means of Chemical Analysis. *Atomic Fluoresence Spectromentry as a Means of Chemical Analysis.* Gainesvile : s.n., 1964, pp. 161-162.

3. *Review of multielement Atomic Spectroscopic Methods.* **J.D. Winefordner, J.J. Fitzgerald, and N. Omenetto.** 5, s.l. : Optica Publishing Group, 1975, Applied Spectroscopy, pp. 369-383.

4. *Generation of Volatile Compounds for Analytical Atomic Spectroscopy.* **Dędina, Jiří.** 2010, Encyclopedia of Analytical Chemistry: Applications, Theory, and Instrumentation.

5. *The comparative verification of calibration curve and background fundamental parameter methods for impurity analysis in drug materials.* **Hiroaki Furukawa, Naoto Ichimaru, Keijiro Suzuki, Makoto Nishino,Jennifer Broughton Johan Leinders and Hirotomo Ochi.** 2017, X-Ray Spectrom, p. 6.

6. *Quantitative X-ray fluorescence analysis: Trace level detection of toxic elemental impurities in drug products by ED-XRF spectromenter.* **Anirban Roy Chowdhury∗, Neelesh Maheshwari, Jigar Soni, Mona Kapil, Tushar Mehta, Amit Mukharya.** 2020, Journal of Pharmaceutical and Biomedical Analysis, p. 7.

7. *Field portable XRF analysis of environmental samples.* **Dennis J Kelnicky, Raj Singhiv.** 2001, Journal of Hazardous Materials, pp. 93-122.

8. *Recent advances in LIBS and XRF for the analysis of plants.* **Gabriel G. A. de Carvalho, *a Marcelo B. B. Guerra,b, Andressa A.,c Cassiana S. Nomura,a.** 2018, J. Anal. At. Spectrom, pp. 919-944.

9. *Inductively Coupled Plasma Mass Spectrometry: Introduction to Analytical Aspects.* **Baxter, Scott C Wilschefski and MatthewR.** 2019, THE CLINICAL BIOCHEMIST REVIEWS , pp. 115-133.

10. *ICP-MS — ICP-MS Instrumentation, ICP-MS Analysis, Strengths and Limitations.* **McMahon, Greg.** 2021, TCHNOLOGY NETWORKS; Analysis and Sepatations, p. 6.

11. *Quadrupole ICP-MS: Introduction to Instrumentation,Measurement Techniques and Analytical Capabilities.* **Jarvis, Kathryn L. Linge and Kym E.** 2019, Back to Basics Review, pp. 445-467.

12. **Adriana Vâlcu, Sterică Baicu.** *Analysis of the Results Obtained in the Calibration of Electronic Analytical Balances.* Mass Laboratory, National Institute of Metrology (INM). Iasi, Romania : Institute of Electrical and Electronic Engineers , 2012. pp. 25-27.

13. *Energy dispersive X-ray fluorescence quantitative analysis of biological samples with the external standard method.* **Patrícia M.S. Carvalho, Sofia Pessanha, Jorge Machado, Ana Luísa Silva, João Veloso, Diogo Casal, Diogo Pais, José Paulo Santos.** 2020, Spectrochimica Acta Part B , p. 8.

14. **United States Environmental Protection Agency.** *METHOD 3050B ACID DIGESTION OF SEDIMENTS, SLUDGES, AND SOILS.* Columbus : ACS American Chemical Society, 1996.

15. *Can field portable X-ray fluorescence (pXRF) produce high quality data for application in environmental contamination research?* **Taylor, Marek Rouillon Mark P.** 2016, Environmental Pollution, p. 10.

16. *Effective energy dispersive X-ray fluorescence method according to ICH Q3D guidelines.* **Johannes Hesper.** 5, Duisburg, Germany : SPECTROSCOPYEUROPE, 2020, Vol. 32.

17. **Burker.** 2. *www.burker.com/hhxrf.* [Online] November 2, 2015. http://ramontxrf.260mb.net/Periodic_Table_and_X-ray_Energies.pdf?i=1.

18. *An assessment of vitamin B12 through determination of cobalt by X-ray fluorescence spectrometry.* **Y. Sunitha *, Sanjiv Kumar.** s.l. : Elsevier, 2021, Radiation Physics and Chemistry, p. 188.

19. *Feasibility of wavelength dispersive X-ray fluorescence spectrometryfor the determination of metal impurities in pharmaceutical products and dietary supplements in view of regulatory guidelines.* **Alexandra Figueiredoa, b,c, Tânia Fernandesa,b, Isabel Margarida Costaa,b,Luísa Gonc¸alvesa,b, José Britoa,.** s.l. : Elsevier, 2016, Journal of Pharmaceutical and Biomedical Analysis, pp. 52–58.

20. *The comparative verification of calibration curve and background fundamental parameter methods for impurity analysis in drug materials.* **Hiroaki Furukawa, Naoto Ichimaru, Keijiro Suzuki, Makoto Nishino, Jennifer Broughton, Johan Leinders and Hirotomo Ochi.** 2017, X-Ray Spectrom, p. 6.

21. —.**Hiroaki Furukawa, Naoto Ichimaru, Keijiro Suzuki, Makoto Nishino, Jennifer Broughton, Johan Leinders, Hirotomo Ochi.** 2017, X-Ray Spectromentry, p. 6.

22. *Energy dispersive X-ray fluorescence determination of uranium in different uranates using Rh Kα scattered peaks for matrix correction.* **S. Sanjay Kumar, Sangita Dhara.** 2022, Spectrochimica Acta Part B: Atomic Spectroscopy, p. 5.

23. *Can XRF scanning of speleotherms be used as a non-distructuve method to isentify poleoflood events in cavaes?* **Martin Finne, Malin Kylander, Meighan Boyd, Hanna S. Sundqvist and Ludvig Lowemark.** Tampa, FL. : International Journal of Speleology, January 2015, International Journal of Speleology, pp. 17-23.

24. **United States Environmental Protection Agency.** *FIELD PORTABLE X-RAY FLUORESCENCE SPECTROMETRY FOR THE DETERMINATION OF ELEMENTAL CONCENTRATIONS IN SOIL AND SEDIMENT.* Columbus : CAS,, 2007.

25. *Direct multielement determination of Cd, Pb, Fe, and Mn in ground coffee samples using energy dispersive X-ray fluorescence spectrometry.* **Jorge S. Almeida, Lucilia A. Meira, Maiara S. Oliveira, Leonardo S. G. Teixeira.** 2020.

26. *Evaluation and calibration of a Field Portable X-Ray Fluorescence spectrometer for quantitative analysis of siliciclastic soils and sediments.* **Timothy C. Kenna, Frank O. Nitsche, Michael M. Herron, Brian J. Mailloux, Dorothy Peteet, Sanpisa Sritrairat, Elizabeth Sands and Joni Baumgarten.** 2011, Journal of Analytical Atomic Spectroscopy., p. 11.